CDK7, CDK9, or CDK11 Inhibition Reduces Neutrophil-Driven Inflammation and Tissue Damage in Experimental Autoimmune Models

Mareile Schlotfeldt[1], Leonie Voss[2], Adrian P. Mansini[3], Daniel Mehlberg[1], Sophia Johannisson[1], Michael Radziewitz[1], Ann-Kathrin Schneider[2], Seyed Mohammad Vahabi[3], Yulu Wang[3], Haley Gainer[3], Jing Li[3], Colin Osterloh[1], Nancy Ernst[1], Remco Visser[4], Gestur Vidarsson[4,5], Frank Petersen[6], Xinhua Yu[6], Ralf J. Ludwig[1,7], Artem Vorobyev[1,7], Kyle T. Amber[3], Anja Lux[2], Katja Bieber[1]

[1]Lübeck Institute of Experimental Dermatology (LIED), University of Lübeck, Lübeck, Germany

[2]Department of Biology, Institute of Genetics, Friedrich-Alexander University (FAU) Erlangen-Nürnberg, Erlangen, Germany

[3]Department of Dermatology, Rush University Medical Center, Chicago, IL, United States

[4]Immunoglobulin Research Laboratory, Sanquin Research, Amsterdam, The Netherlands

[5]Department of Biomolecular Mass Spectrometry and Proteomics, Utrecht Institute for Pharmaceutical Sciences and Bijvoet Center for Biomolecular Research, Utrecht University, Utrecht, The Netherlands

[6]Priority Area Asthma and Allergy, Research Center Borstel, Airway Research Center North, German Center for Lung Research, Borstel, Germany

[7]Department of Dermatology, University of Lübeck, Lübeck, Germany

Abstract

Cyclin-dependent kinases are involved in basic cellular processes like regulation of cell-cycle progression and transcription. However, recent data also indicate a specific role in terminally differentiated neutrophils by promoting reactive oxygen species (ROS) release, degranulation, neutrophil extracellular trap (NET) formation, or apoptosis. Thus, we investigated the effect of pharmacological CDK inhibition on IC-activated neutrophil functions. Inhibitors targeting CDK1, 2, 4/6, 7, 9, 11, and 12 showed effects on different neutrophil functions (surface activation marker expression, ROS release, adhesion, apoptosis) *in vitro*. To analyse the inhibitors in a more translational approach, we proceeded with the systemic application of the effective inhibitors in a murine antibody transfer-induced local EBA model. In this predominantly neutrophil-driven model, we observed a reduction of disease severity upon treatment with CDK7, 9, or 11 inhibitors. Inhibiting these CDKs with topical THZ2, MC180295, or OTS964 also improved the clinical phenotype. Therefore, the most efficient inhibitor, MC180295, was validated in two other IC-mediated models of autoimmune disease: Serum-transfer arthritis, which also, but not exclusively depends on neutrophils and ITP, which is considered neutrophil-independent. Here, an effect in STA was observed, but not in ITP. Hence, we show the therapeutic potential of CDK7, 11, and especially 9 inhibition in IC-driven neutrophil-mediated diseases such as RA and EBA.

Introduction

Cyclin-dependent kinases (CDKs) are a group of serine-threonine kinases that were discovered for their involvement in the regulation of the eukaryotic cell cycle (Nurse et al. 1976; Beach et al. 1982; Malumbres 2014). They are crucially contributing to the correct replication and subsequent separation of the chromosomal DNA during mitosis (Nurse 2000). CDKs are highly conserved across eukaryotes, from yeast to mammals (Lee and Nurse 1987). They were termed for their critical interaction with specific regulatory protein binding partners, the cyclins (Evans et al. 1983). The latter are expressed in a cyclic fashion during the cell cycle, while the CDKs themselves are stably expressed throughout the cell cycle (Malumbres 2014). There are 20 CDKs and 29 cyclins described in mammals (Cao et al. 2014), as well as other regulating proteins such as intrinsic CDK inhibitors (CKI) (Bury et al. 2021). But activation of CDKs not only requires the interaction with a cyclin, also phosphorylation at a specific tyrosine residue in the activation loop is necessary (Draetta and Beach 1988; Russo et al. 1996). This phosphorylation of at least CDK1/2/4/6/9/12/13 is mediated by the CDK-activating kinase (CAK) complex (Pluta et al. 2024), consisting of CDK7,cyclin H and MAT1 (Tassan et al. 1994; Solomon et al. 1992; Fisher and Morgan 1994). Importantly, CDK inactivation is regulated by phosphorylation (Parker and Piwnica-Worms 1992) or binding of CKIs (Jeffrey et al. 2000; Pavletich 1999).

However, there is rising evidence that CDKs not only play a role in direct cell cycle regulation, but also in regulating the RNA pol II transcription cycle (Lim and Kaldis 2013; Pluta et al. 2024). It was claimed that there are two groups: the cell-cycle CDKs (subfamilies CDK1, 2, 3, 4, and 6) and the transcriptional CDKs (subfamilies CDK 7, 8, 9, 10, 11, 12, and 13) (Cao et al. 2014). The remainder is referred to as atypical CDKs, although these kinases are insufficiently characterised (Pellarin et al. 2025). Though this may be a helpful concept, this dichotomy is probably oversimplified. More and more studies demonstrate roles for traditional cell-cycle CDKs in transcriptional regulation and vice versa (Nilson et al. 2015; Peissert et al. 2020; Leitch et al. 2012; Lim and Kaldis 2013).

Considering that CDKs are not only expressed in proliferating cells, but also in terminally differentiated cells like neutrophils (Syahirah et al. 2022), it seems a reasonable assumption that their role extends beyond mere cell cycle regulation. Neutrophils are known as the first line of defence against pathogens (Aroca-Crevillén et al. 2024). Once activated, they are recruited to the tissue of interest and are activated by the binding of immune complexes (IC) to their fragment crystallisable gamma receptors (FcγR). Downstream kinase signalling cascades are activated, triggering effector functions such as reactive oxygen species (ROS), protease and cytokine release to kill the invading pathogens in a controlled manner. Subsequently, the neutrophils are cleared mostly by macrophages under inflammatory conditions (Savill et al. 1989; Greenlee-Wacker 2016). Notably, a role for several CDKs in regulating neutrophil functions has been described: CDK2 is involved in migration (Hsu et al. 2019), CDK4/6 in NET formation (Amulic et al. 2017), CDK5 in degranulation (Rosales et al.

2004), and CDK7/9 in apoptosis (Leitch et al. 2012; Wang et al. 2012). Still, little is known about the distinct functions of different CDKs in direct comparison, and most studies rely on broad-range CDK inhibitors (CDKi). Moreover, their potential involvement in FcγR-mediated signalling remains largely unexplored, representing a significant gap in our understanding of CDK biology.

An increasing number of studies points towards a relevance of CDKs in various human disorders, underlining the need for a better comprehension of these kinases. Deregulated CDK activity has been shown to be associated not only with e.g. neurodegenerative diseases (Bajaj et al. 1998) and cancer (Pellarin et al. 2025), but also with autoimmune diseases like rheumatoid arthritis (RA) (Yik et al. 2014) or systemic lupus erythematosus (SLE) (Wu et al. 2016). In contrast to infectious diseases however, there is no pathogen in autoimmunity, but autoantibodies develop against self-antigens due to a break of tolerance. To unravel the function of CDKs in the context of neutrophil-mediated FcγR-dependent signalling, we investigated the kinase signalling pathways upon immune-complex stimulation in human neutrophils *in vitro*. Furthermore, we chose three well-established murine *in vivo* models of autoimmune diseases: Epidermolysis bullosa acquisita (EBA), serum-transfer arthritis as a model for RA, and immune thrombocytopenia (ITP). EBA belongs to the group of pemphigoid diseases (PD), which is a group of rare autoimmune bullous diseases characterised by autoantibodies targeting structural proteins at the dermal-epidermal junction. More specifically, the autoantigen in EBA is collagen VII (COL7) (Woodley et al. 1988). Neutrophils are the central effector cells in PD (Liu et al. 1997; Matsumoto et al. 2024), causing the uncontrolled release of inflammatory mediators. Thereby, tissue damage occurs, causing the degradation of the dermal-epidermal adhesion complex and subepidermal split formation (Chiriac et al. 2007; Bieber et al. 2016). Clinically, patients present with pruritus, erosions, and tense, painful blisters on different sites of the body, e.g. trauma-prone areas or the extensor skin surface (Schmidt and Zillikens 2013). Currently, the patients are most commonly treated with systemic corticosteroids, bearing a high risk for side effects due to general immunosuppression (Koga et al. 2019; Kridin et al. 2019).

Another more prevalent neutrophil-dependent autoimmune disease with the need for novel therapeutic options is RA, modelled by STA (Christensen et al. 2016). In contrast to EBA, neutrophils do play a critical role in pathogenesis (Wipke and Allen 2001; Wright et al. 2014), but other cell types like macrophages (Solomon et al. 2005) or mast cells (Lee et al. 2002; Nigrovic et al. 2007) are crucially involved in the effector phase. Joint inflammation, bone and cartilage destruction are major hallmarks of RA (McInnes and Schett 2011).

Conversely, immune thrombocytopenia is also IC-driven, but neutrophil-independent, which makes it interesting to contrast these three models. In ITP, autoantibodies target platelets leading to their phagocytosis mainly by macrophages or dendritic cells and thus to platelet depletion (Zufferey et al. 2017).

Since kinases are generally well-druggable targets (Schwartz and Murray 2011; Zarrin et al. 2021) and considering that there are several CDK inhibitors already on the market, e.g. for cancer treatment (Cicenas and Valius 2011), a potential repurposing of the inhibitors could accelerate the process of clinical approval. Thus, the characterisation of CDK signalling cascades in neutrophils can help to identify potential therapeutic targets for PD, but also potentially for other neutrophil-driven autoimmune diseases like RA. This could provide targeted treatment options to the patients and therefore drastically ameliorate the safety profile of the therapy.

Material and methods

Sampling of human biomaterials

Whole blood was obtained from healthy volunteers after written informed consent. All experiments using human samples were approved by the local ethics committee (AZ #20-463, University of Lübeck, Lübeck, Germany) and were performed in accordance with the Declaration of Helsinki.

Chemicals

All standard chemicals were supplied by Carl Roth (Karlsruhe, Germany) or Sigma-Aldrich (Taufkirchen, Germany). CDKi were supplied by Selleck Chemicals (Houston, Texas, USA) or MedChemExpress (Monmouth Junction, New Jersey, USA). For *in vitro* assays, 10 mM CDKi was dissolved in DMSO and further diluted to final concentrations of 10 µM, 1 µM, 01 µM, and 0.01 µM. DMSO at a final concentration of 0.1 % was included in the controls. For *in vivo* experiments, CDKi were prepared as stated in table 1. The respective vehicle only served as the respective control.

Table 1. CDKi used in this study.

substance	main target	vehicle	dosage [mg/kg]	route	fre-quency	IC_{50}/*Kd*/Ki [nM]
Ro-3306	CDK1	10 % DMSO/ 30 % PEG-300/ 10 % Tween-80	4	p.o.	daily	*20*
OTS964	CDK11B	5 % DMSO, 40 % PEG300, 5 % Tween-80	40	p.o.	daily	40
Palbociclib HCl	CDK4/6	sodium lactate buffer (50 mmol/L, pH 4.0)	100	p.o.	daily	9
THZ1 2HCl	CDK7	10 % DMSO/ 90 % 5 % dextrose in water	10	i.p.	twice daily	3.2
THZ2	CDK7	10 % DMSO in D5W, 5 % dextrose in water	10	i.p.	daily	13.9

MC180295	CDK9	5 % DMSO/ 40 % PEG-300/ 5 % Tween-80/ 50 % water	20	i.p.	daily	5
LY3143921 hydrate	CDC7	-	-	-	-	?
BMS-265246	CDK1/2	-	-	-	-	6
BSJ-4-116	CDK1/2	-	-	-	-	?
Purvalanol B	CDK1/2/5	-	-	-	-	6
SR-4835	CDK12/13	-	-	-	-	4.9
K03861	CDK2	-	-	-	-	9.6
AS2863619	CDK8/19	-	-	-	-	0.6
BAY1251152	CDK9	-	-	-	-	3

Isolation of human immune cells by magnetic activated cell sorting (MACS)

For the isolation of human neutrophils by MACS, blood from healthy young (< 30 y) donors was drawn into citrate blood collection tubes. After 1:2 dilution with 1 % (w/v) polyvinyl alcohol and sedimentation for 25 min, the supernatant (up to 40 mL) was transferred on top of a layer of 8 mL of Ficoll Paque PLUS (Cytiva, Marlborough, Massachusetts, USA). Density gradient centrifugation (Skoog and Beck 1956) was performed for 24 min at 850 g and room temperature (RT) without brake. The lymphocyte layer was processed for B and $CD4^+$ T cell isolation, whereas the granulocyte pellet was used for neutrophil and eosinophil purification. The lymphocyte layer was resuspended in PBS and centrifuged at 300 g for 10 min at 4 °C for platelet removal. Another washing step with PBS was performed at 400 g for 10 min at 4 °C. Next, the purified lymphocytes were subjected to MACS according to the manufacturer's instructions using the $CD4^+$ T cell isolation kit (130-096-533, Miltenyi Biotec, Bergisch Gladbach, Germany) and the B cell isolation kit II (130-091-151, Miltenyi Biotec). B and $CD4^+$ T cell purities were assessed by flow cytometry and were > 80 %.

For erythrocyte lysis, the granulocyte pellet was resuspended in distilled water, mixed for 45 s, and then neutralised with 2x PBS. Two washing steps with PBS were performed for 10 min at 300 g and RT. Subsequently, the polymorphonuclear leukocytes (PMNs) were subjected to eosinophil removal by

MACS according to the manufacturer's instructions (130-092-010, Miltenyi Biotec). Neutrophil and eosinophil purities were assessed by flow cytometry and were > 96 %.

Bulk RNA sequencing

For bulk RNA sequencing (RNAseq), 100,000 MACS-purified neutrophils from healthy volunteers were sampled and frozen at -80 °C in 1 mL Trizol (Invitrogen, Waltham, Massachusetts, USA). An equal number of cells from each donor was stimulated for 6 h at 37 °C and 5 % CO_2 with immobilised IC consisting of human COL7E-F and anti-human COL7 IgG1 as previously described before (Zillikens et al. 2021). All samples were sent to Single Cell Discoveries (Utrecht, The Netherlands) for RNA extraction and sequencing. Data analysis was performed in RStudio (Posit Software, Boston, Massachusetts, USA; version 2024.12.1) as previously described (Stüssel et al. 2020). Differentially expressed genes were identified using DESeq2 (Love et al. 2014), where $p_{adj} < 0.1$ was considered significant. Gene set enrichment analysis was conducted using ClusterProfiler referring to the Gene Ontology (GO) database (The Gene Ontology Consortium et al. 2023; Ashburner et al. 2000). The data for this study have been deposited in the European Nucleotide Archive (ENA) at EMBL-EBI under accession number PRJEB103987 (https://www.ebi.ac.uk/ena/browser/view/PRJEB103987).

Human polymorphonuclear granulocyte (PMN) purification

For ROS release assay, flow cytometry, adhesion assay, and qRT-PCR, PMNs were isolated from EDTA-treated human whole blood performing a PolymorphPrep™ (Serumwerk Bernburg AG, Bernburg, Germany) density gradient centrifugation as previously described (Stüssel et al. 2020; Ghorbanalipoor et al. 2024; Zillikens et al. 2021). The cells were diluted to $4x10^5$ cells/mL in 1 % (w/v) bovine serum albumin (BSA) in PBS. Neutrophil purity was assessed by flow cytometry for all experiments and was higher than 90 % for all samples.

Real-time quantitative reverse transcription polymerase chain reaction (qRT-PCR)

For gene expression analysis by qRT-PCR, human PMNs were stimulated with human COL7E-F anti-human COL7 IgG1 IC for 6 h at 37 °C and 5 % CO_2 as stated above. Alongside unstimulated PMNs, eosinophils, B cells and $CD4^+$ T cells isolated by MACS as described above, the cells were collected with a cell scraper in PBS and centrifuged for 7 min at 700 g and RT. The lysates were resuspended in 700 µL RLT buffer (Qiagen, Hilden, Germany) and frozen at -80 °C until RNA extraction. RNA extraction was performed using the innuPREP RNA Mini Kit 2.0 (Analytik Jena, Jena, Germany) according to the manufacturer's instructions. Any remaining RNA was digested with DNase I (Sigma-Aldrich). cDNA was synthesised using the RevertAid Reverse Transcriptase (Thermo Fisher Scientific, Waltham, Massachusetts, USA) according to the manufacturer's instructions. TaqMan™ gene expression assays (see table 2) were purchased from Thermo Fisher Scientific and used according to the manufacturer's instructions. qRT-PCR was performed on an Applied Biosystems

7900HT Fast Real-Time PCR System (Thermo Fisher Scientific). The results were analysed using the $2^{-\Delta\Delta Ct}$ method (Livak and Schmittgen 2001) and normalised to the mean values of the housekeeping genes (Zhang et al. 2005).

Table 2. TaqMan™ gene expression assays used for qRT-PCR.

	Catalogue no.	Assay ID	Gene symbol
CDKs	4453320	Hs00938777_m1	*CDK1*
	4453320	Hs01548894_m1	*CDK2*
	4448892	Hs01077186_g1	*CDK3, TEN1-CDK3*
	4453320	Hs00364847_m1	*CDK4*
	4453320	Hs00358991_g1	*CDK5*
	4453320	Hs01026371_m1	*CDK6*
	4448892	Hs00361486_m1	*CDK7*
	4448892	Hs00992501_g1	*CDK8*
	4448892	Hs00977896_g1	*CDK9*
	4448892	Hs02341397_m1	*CDK11A*
	4448892	Hs07291776_gH	*CDK11B*
	4448892	Hs00901732_m1	*CDK12*
	4448892	Hs00953418_m1	*CDK14*
	4448892	Hs01039930_g1	*CDK19*
	4453320	Hs00177487_m1	*CDC7*
housekeeping genes	4331182	Hs01060665_g1	*ACTB*
	4331182	Hs02786624_g1	*GAPDH*
	4331182	Hs02800695_m1	*HPRT*
	4331182	Hs00272002_m1	*GNB2L1*

Reactive oxygen species (ROS) release assay

Plates were coated with IC consisting of human COL7 E-F at 2.5 µg/mL and anti-human COL7 IgG1 at 1.8 µg/mL as previously described (Recke et al. 2014; Zillikens et al. 2021). PMNs were added at $2x10^5$ cells per well in the presence or absence of CDKi. Only antibody (with cells), only antigen (with cells), or only cells served as negative controls, while PMA at 10 nM served as positive control. DMSO was adjusted to a final concentration of 0.01 %. All samples were measured in duplicates. Luminol was automatically injected into each well to reach a final concentration of 90 µg/mL, and luminescence was measured for 2 h every 2 min at 37 °C in a GloMax® Discover microplate reader

(Promega, Walldorf, Germany). The area under the curve (AUC) was calculated, and the results were normalised to IC-stimulated cells without CDKi.

Adhesion assay

PMN adhesion was investigated using impedance-based measurements as described before (Yu et al. 2018; Yang et al. 2023). A 96-well E-plate (Agilent, Santa Clara, California, USA) was coated with IC as described for the ROS release assay. Inhibitor solutions were prepared and added to the plate before $2x10^5$ cells were transferred to each well. Impedance was measured in an xCELLigence real-time cell analysis device (Agilent) every 2 min for 120 min expressed in arbitrary units as cell index. Data analysis was performed as for the ROS release assay.

Flow cytometry

Human PMNs were isolated as previously described and stimulated with ICs, prepared in the same manner as for the ROS release assay, for 2 hours at 37 °C and 5 % CO . Subsequently, they were stained for the flow cytometric analysis of the following surface markers using standard flow cytometry procedures: CD14 (clone HCD14), CD16 (clone 3G8), CD18 (clone 1B4/CD18), CD45 (clone HI30), and CD62L (clone DREG-56), CD193 (clone 5E8). Viability was assessed by Annexin V (B266195) and Zombie NIR staining (B308933) (Stüssel et al. 2020). Analyses for activation markers were performed on FSC-SSC gated $CD45^+$ singlets. Annexin V^- Zombie NIR^- cells were considered viable, Annexin V^+ Zombie NIR^- cells were considered apoptotic. All dyes were purchased from BioLegend (San Diego, California, USA). Measurements were performed on a MACSQuant® Analyzer 10 (Miltenyi Biotec) and analysis was conducted using MACS Quantify software (version 2.13.3, Miltenyi Biotec).

Study approval

Animal experiments were approved by local authorities of the Animal Care and Use Committee (government of Schleswig-Holstein and government of Lower Franconia) and the Institutional Animal Care and Use Committee at Rush University. All experiments were performed by certified personnel (AZ 108/08-15, AZ 97-11/20 and 55.2.2-2532-2-2085) following the ARRIVE guidelines.

Animal experimentation

C57BL/6J mice (Charles River, Wilmington, Massachusetts, USA) were bred in a specific pathogen–free environment and provided standard mouse chow and acidified drinking water *ad libitum*. Mice of both sexes, aged 8 to 14 weeks, were used for experimental EBA models with clinical examinations performed under anaesthesia, using intraperitoneal (i.p.) administration of a ketamine (75 mg/kg, Sigma-Aldrich) and medetomidine (1 mg/kg, Vetoquinol, Ismaning, Germany) mixture, antagonised after ca. 30 min by atipamezole (5 mg/kg, Vetoquinol). On the final day, the mice were anaesthetised

using 15 mg/kg xylazine (Sigma-Aldrich) and 100 mg/kg ketamine. STA and ITP models were performed with female C57BL/6J aged 8 weeks. For narcosis, isoflurane was used and mice were killed by CO_2.

Local antibody-transfer induced experimental EBA

Specific anti–mouse COL7^{C} IgG from rabbit serum was isolated as described previously (Bieber et al. 2017; 2016; Sitaru et al. 2005; Kasprick et al. 2019). CDKi were administered as indicated in table 1 at 100 µL/20 g mouse for systemic treatment or for topical treatment MC180295 was applied at 65 µg/100 µL in acetone/DMSO (20:1) per ear daily, beginning one day before the anti–mouse COL7^{C} IgG injection and was performed daily throughout the 5-day experiment. Vehicle-treated mice served as controls in all cases. Experimental EBA was induced by ear-base injection with 100 µg rabbit anti–mouse COL7 ^{C} IgG. The mice were evaluated clinically every day, and the percentage of ear thickness was assessed using a Mitutoyo 7301 dial thickness gauge (Neuss, Germany) by a blinded person, as well as the affected ear surface area. Ears were collected on the final day of the experiment, and half of each ear was embedded in 4 % PBS-buffered paraffin or frozen in liquid nitrogen and stored at -80 °C. Paraffin-embedded samples were subjected to hematoxylin-eosin (H&E) staining. Split formation, cell infiltration, and epidermal thickness were evaluated as described before (Gross et al. 2024). Frozen samples were used for direct immunofluorescence staining, detecting IgG and C3 deposits as described previously (Bieber et al. 2016).

Serum-transfer arthritis (STA)

Serum transfer arthritis (STA) was induced by injection of arthritogenic KBxN serum in female C57BL/6J mice at 10 µL/g bodyweight as described before (Seeling et al. 2023). Before and after arthritis induction, mice were treated daily with 20 mg/kg body weight MC180295 or vehicle control p.o. The severity of joint swelling was monitored to evaluate clinical disease over the course of seven days. Peripheral blood was collected retro-orbitally on day 0 and day 7, and inflammatory cytokines were quantified in the serum by LegendPlex multiplex assay (Mouse Inflammation 13-plex, BioLegend) as a parameter of systemic inflammation. On day 7, mice were sacrificed, and forelegs were prepared for histological analysis. H&E staining was performed to evaluate inflammatory infiltrates and Safranin-O staining to assess bone and cartilage damage, as described previously (Seeling et al. 2013; 2023). Stained sections were evaluated by light microscopy using a Zeiss Axiovert 200 microscope and the AxioVision LE4.6 software (Olympus Life Science, Waltham, Massachusetts, USA).

Immune thrombocytopenia (ITP)

Platelet depletion in the presence of kinase inhibition was assessed in female C57BL/6J mice. Platelet depletion was induced by injection of 0.35 µg/g anti-platelet IgG2c (clone 6A6) as described (Wöhner

et al. 2024). Treatment with vehicle control or MC180295 (20 mg/kg body weight i.p.) was performed 24 h and 4 h before the induction of platelet depletion. Platelet counts in peripheral blood were assessed immediately before 6A6-IgG2c injection, and at 4 h and 24 h post-injection in peripheral blood collected retro-orbitally. Platelet counts were determined using an ADVIA® 2120i hematocytometer (Siemens Healthineers, Erlangen, Germany).

Statistical analysis

Data were analysed using Prism 10.4.1 (GraphPad Software, San Diego, USA). For all *in vitro* assays, Kruskal-Wallis test with Dunn's multiple comparisons test was performed if not indicated differently. Dose response curves and IC_{50} values were calculated using the non-linear fit inhibitor vs. response (three parameters) function or for EC_{50} values using the agonist vs. response (three parameters) function where an activating response was observed. For all *in vivo* experiments, two-way ANOVA or mixed-effects analysis (in the case of missing values) with Šidák's multiple comparisons test were performed unless stated differently. A value of $p \leq 0.05$ was considered significant. The data are displayed as Tukey box-and-whisker plots or else as mean ± standard deviation unless described differently.

Data availability

The data that support the findings of this study are available from the corresponding author upon reasonable request.

Results

Fourteen CDKs are expressed at mRNA level in human neutrophils and expression of CDK2 and 4 changes upon IC stimulation

CDKs are essential to drive cell cycle progression in proliferating cells (Pellarin et al. 2025). However, at least certain CDKs seem to be functionally relevant also in terminally differentiated cells like neutrophils (Amulic et al. 2017; Hsu et al. 2019; Leitch et al. 2012; Rosales et al. 2004). Since there are conflicting data published on this topic (Leitch et al. 2012; Amulic et al. 2017), we first set out to clarify which CDKs and regulating proteins are expressed at mRNA level in human neutrophils. Therefore, an RNAseq experiment on neutrophils from healthy volunteers was performed. In addition, neutrophils were stimulated with immobilised ICs for 6 h and compared to the unstimulated neutrophils to reveal any transcriptional changes (Fig. 1A). From the 20 CDKs that are overall expressed in humans, we found 14 CDK transcripts (both paralogues of *CDK11*) expressed in unstimulated neutrophils and 6 significantly changed by IC stimulation. While *CDK13* and *19* expression was downregulated after 6 h, *CDK2*, *4*, *7*, and *12* expression was upregulated. Regarding cyclins, 16 out of 29 genes were expressed. On the one hand, the CDKs that have best established roles in direct regulation of the cell cycle, *CDK1*, *2*, *4*, and *6*, were all except *CDK1* detected by

RNAseq. The gene expression of *CDK2* and *4* was induced upon IC stimulation. In addition, their partner cyclins were also measured except cyclin E (*CCNE*), which binds to CDK2 during late G1 phase to promote G1-S transition. Cyclin A (*CCNA*) was unchanged after IC stimulation, whereas cyclin B (*CCNB*) and D (*CCND*) showed an increased expression. On the other hand, the transcriptional kinases *CDK7*, *9*, *12*, *13* and *19* were observed, but not *CDK18*. Their cyclin binding-partners were all detected with cyclin H (*CCNH*) and T (*CCNT*) elevated upon IC treatment. In addition, the gene expression of other CDK-regulating proteins like RB1, EP300 or MED12/13 was significantly elevated after IC stimulation (Fig. 1B). GO pathway analysis revealed an activation of granulocyte-specific pathways and a suppression of metabolic pathways (Fig. 1C).

qRT-PCR confirms the expression of 14 CDKs from RNAseq in human PMNs

To validate the results from RNAseq, an independent qRT-PCR experiment was performed on unstimulated and IC-stimulated human PMNs. All tested *CDKs* were detected, although *CDK1*, *3*, *5*, *6*, *8*, *11A*, and *CDC7* were expressed at a relatively low level ($2^{-\Delta\Delta Ct} < 0.1$) under both conditions. The expression of *CDK2* and *4* was increased more than threefold or sixfold, respectively, after 6 h IC stimulation, while *CDK9* expression decreased by half and *CDK19* expression by approximately 70 %. *CDK3* and *CDK11B* showed a trend to be reduced (both $p = 0.0556$), but all other *CDKs* remained unaffected by IC stimulation (Fig. 2A). The results support the RNAseq data which also indicate an IC-mediated induction of *CDK2* and *4* transcription, but a reduction of CDK9 and 19 transcription (see section above). For comparison with proliferating cells, B and $CD4^+$ T cells were also analyzed in qRT-PCR (Fig. 2B). Strikingly, *CDK1*, *2*, *4*, *5*, *6*, *8*, and *CDC7* were expressed at higher levels in B and/or T cells, whereas *CDK4*, *9*, *11B*, *14*, and *19* were increased in PMNs.

Pharmacological inhibition of multiple specific CDKs partially protects *in vitro* from neutrophil effector functions in a dose-dependent manner

To functionally evaluate the role of CDKs in neutrophil kinase signalling, we tested selected CDKi in several neutrophil assays, covering multiple steps from neutrophil activation to cell death. Therefore, COL7-anti-COL7-IgG1 ICs were immobilised on plates, incubated with PMNs from healthy donors and the respective experiment was performed. The surface expression of CD62L, an L-selectin which is shed upon neutrophil activation (Griffin et al. 1990; Kuhns et al. 1995), was analysed first. The CDK9i MC180925 (Fig. 3), CDK1i Ro 3306, and CDK7i THZ1 2HCl (Fig. S1) significantly reduced CD62L shedding, while the other inhibitors tested did not (Fig. 3, S1). CDK7 inhibition with THZ2 reduced CD18 expression (Fig. 3), which is a β2-integrin responsible for neutrophil adhesion (Arnaout 2016). Similar effects were observed for Ro 3306 and THZ1 2HCl (Fig. S2). Subsequently, adhesion measurements demonstrate a significant reduction only for THZ2 (Fig. 3, S3). Furthermore, THZ2,

MC180295, OTS964, Ro 3306, BMS-265246, K03861, palbociclib HCl, THZ1 2HCl, and BAY1251152 inhibited ROS release (Fig. 3, S4). Regarding apoptosis, a significant increase was measured for THZ2, OTS964, and BSJ-4-116 (Fig. 3, S5). For BMS-265246 and AS2863619, statistical significance was reached, however, the values did not exceed those of the negative controls (Fig. S5). Although viability was significantly lower at especially at 10 µM, more than 99 % of the cells remained viable in all cases (Fig. 3, S6). Thus, the ROS release assay shows the most promising results, highlighting the inhibitory potential of especially THZ2, MC180295 and OTS964 in combination with the other *in vitro* experiments.

Both systemic and topical treatment with CDK7, 9 or 11 inhibitors reduces disease severity in the local antibody-transfer induced EBA model

Following the successful *in vitro* validation of the selected CDKi, a local antibody-transfer induced EBA model was performed to test these compounds as systemic treatment (Fig. 4A). CDK9 inhibition by MC180295 completely prevented disease induction, which is exemplified by representative images showing the ameliorated clinical presentation of the mice, the reduced inflammation in the H&E staining as well as IgG and C3 deposition along the dermal-epidermal junction (Fig. 4B). The AESA was significantly reduced starting at day 1 and increasing further until day 3, which is also reflected by the H&E score (Fig. 4C). CDK7 inhibition by both THZ2 (Fig. 4D) and THZ1 2HCl (Fig. 4E) reduced the affected ear surface area, but with slightly more variability between the individuals. Systemic OTS964 treatment also ameliorated the disease severity, but the H&E score did not change significantly between the treated and the control mice (Fig. 4F). However, treatment with Ro 3306 and palbociclib HCl had no significant effect (Fig. S7).

The most promising inhibitors from the systemic treatment in local antibody-transfer induced EBA were selected for topical treatment in the same model. THZ2 was chosen over THZ1 HCl since both inhibit CDK7, but THZ2 showed better results *in vitro* and almost completely protected from disease development *in vivo*. All three inhibitors tested prevented disease induction when applied topically (Fig. 4E).

CDK9 inhibition with MC180295 is beneficial in neutrophil-dependent STA, but not in neutrophil-independent ITP

The CDKi that showed the most prominent effect in the local antibody-transfer induced EBA model, MC180295, was validated in two other IC-driven models with less prominent neutrophil involvement, namely STA and ITP. In STA (Fig. 5A), systemic treatment with MC180295 significantly reduced the disease score starting at day 5, continuing until day 7 (Fig. 5B). On the molecular level, this was reflected on the one hand by Safranin-O staining to visualise cartilage damage by proteoglycan

degradation in the untreated mice. On the other hand, H&E staining showed immune cell infiltration in the controls, but not or to a lesser extent in the treated mice (Fig. 5C). Out of 13 cytokines tested in the serum, 2 were significantly changed on the final day between the two groups. Both IL-6 and IL-10 were reduced on day 7 in the MC180295-treated group compared to the control group. All other measured cytokine levels were not affected on day 7 or day 0 (Supplemental Table 2).

In contrast to STA, ITP (Fig. 5E) does not primarily depend on neutrophils. Here, prophylactic treatment with MC180295 did not show any effects on platelet count 24 h after platelet depletion (Fig. 5G), demonstrating the variable effect of CDKi in the different disease models.

Discussion

IC-induced FcγR-mediated kinase signalling plays a major role in intracellular signal transduction by neutrophils under pathological conditions, e.g., in autoimmune diseases such as EBA or RA. However, the role of CDKs in neutrophils is largely unknown. A small number of studies have reported the expression of CDKs on protein level and suggested functional relevance in these cells (Amulic et al. 2017; Leitch et al. 2012; Rossi et al. 2006). To the best of our knowledge, we show in the present study for the first time a comprehensive, functional analysis of IC-triggered FcγR-dependent kinase signalling using a variety of specific CDKi. Fig. 6 summarises our main findings.

Interestingly, we identified multiple CDKs as expressed on RNA level and found that transcription may change in IC-stimulated neutrophils. The expression of the two traditional cell-cycle CDKs *CDK2* and *CDK4* increased, whereas the expression of the two transcriptional CDKs *CDK9* and *CDK19* decreased. These trends are clearly supported by our qRT-PCR analysis in an independent dataset. Furthermore, the qRT-PCR data highlight the higher expression of *CDK9*, *11B* and *19* in neutrophils compared to B and $CD4^+$ T cells, making them especially promising targets in neutrophil-dependent diseases. The trends concerning gene expression levels in unstimulated cells found in our RNAseq and qRT-PCR analyses are in line with publicly available RNAseq data of unstimulated neutrophils sorted by flow cytometry from six healthy donors (Uhlén et al. 2015, Human Protein Atlas proteinatlas.org). Several CDKs like CDK2, 4, and 11 were also detected in a kinase activity measurement of IC-stimulated PMNs (Zillikens et al. 2021).

Since CDKs only become fully active after binding to their cyclin binding partners, we also examined cyclins in our RNAseq analysis. Most prominently, we found both CDK7 and its binding partner cyclin H significantly increased upon IC activation. Strikingly, *MNAT1* (MAT1 RNA) was not detected, suggesting the requirement of a phosphorylation-dependent activation of CDK7 (Harper and Elledge 1998; Fisher et al. 1995).

Furthermore, several regulators of CDKs were differentially expressed upon IC stimulation in human neutrophils, hence adding another layer of complexity to the regulation of CDKs in autoimmune disease. Both *MED12* and *13* were transcribed more, possibly promoting the formation of a transcriptional pre-initiator complex after association with CDK8/19 and cyclin C (Donner et al. 2010). Moreover, regulators of chromatin remodelling required for transcriptional activation like *RB1* (Sanidas et al. 2024) and *EP300* (Delvecchio et al. 2013; Ogryzko et al. 1996) were detected at higher RNA levels in stimulated cells.

In addition to the analysis focusing on CDKs and their regulators, we performed a GO pathway analysis for the enriched gene sets from unstimulated versus IC-stimulated neutrophils. Interestingly, our pathway analysis revealed that many metabolic pathways including ATP synthesis or catabolic processes are suppressed, while immune pathways such as granulocyte migration, chemokine and cytokine pathways were activated.

Thus, we hypothesised that targeting CDKs by specific small-molecule inhibitors might reduce neutrophil effector functions in IC-stimulated neutrophils *in vitro* and consequently disease severity in IC-driven neutrophil-dependent models of autoimmune disease *in vivo*. Although there are multiple studies published on CDK inhibition in different contexts, they are rarely focussed on neutrophils and utilise relatively unspecific CDKi. However, pan-CDK inhibition is often associated with severe side effects (Zhang et al. 2021). Here, we therefore chose more specific CDK inhibitors to investigate their role on neutrophil functions upon IC activation.

Hence, we analysed several functions that are critical for neutrophil recruitment as well as apoptosis. As several studies suggest that ROS release might be a predictor of *in vivo* efficacy in experimental EBA (Stüssel et al. 2020; Zillikens et al. 2021; Ghorbanalipoor et al. 2024; Samavedam et al. 2018), all CDKi that significantly reduced ROS release were tested as systemic treatment in the local antibody transfer-induced EBA model (Ro 3306, palbociclib HCl, THZ1 2HCl, THZ2, OTS964). Moreover, inhibition of CDK1, 2, 4/6, 7, 9, or 12 influenced other neutrophil functions such as expression of the surface activation markers CD18 and CD62L, and adhesion, highlighting a role for CDKs in neutrophil recruitment and activation. Viability was only slightly influenced, with values still in the range of the negative controls. Moreover, some inhibitors (THZ2, OTS964, BSJ-4-116) increased apoptosis, which is a highly controlled form of cell death leaving the cell membrane intact (Savill et al. 1989). Partly in line with our data, for CDK7 and 9 in neutrophils (Leitch et al. 2012; Wang et al. 2012), and CDK11 in Chinese Hamster Ovary cells and T-cell lines (Lahti et al. 1995) a role in regulating apoptosis has been already suggested. This may protect the tissue from toxic substances like ROS which are released during alternative forms of cell death and has been described as a potential mechanism of action of CDKi (Leitch et al. 2009; Rossi et al. 2006). Indeed, THZ2 and OTS964 increased apoptosis while reducing ROS. However, other inhibitors reduced ROS release without affecting apoptosis (Ro 3306, K03861, palbociclib HCl, THZ1 2HCl, BAY 1251152),

implicating the involvement of different mechanisms or signalling pathways. Interestingly, CDK9 inhibition by MC180295 or BAY 1251152 did not significantly influence apoptosis, whereas CDK9 inhibition by flavopiridol resulted in apoptosis induction (Wang et al. 2012). Thus, this indicated an inhibitor-specific, probably synergistic effect caused by targeting several CDKs at once with flavopiridol. As delayed apoptosis is a feature of RA (Wright et al. 2014), CDK inhibition might be a reasonable approach in this context.

Subsequently, the most promising CDKi were applied systemically in the local antibody-transfer induced EBA model. Here, inhibition of CDK7 by THZ1 2HCl or THZ2, CDK9 by MC180295, or CDK11 by OTS964 were found to significantly reduce the disease severity. Inhibition of CDK1 with Ro 3306 or CDK4/6 with palbociclib HCl, in contrast, did not reduce the affected ear surface area. Although palbociclib HCl showed promising effects *in vitro* and is licenced as treatment for breast cancer, where it improves the neutrophil-to-lymphocyte ratio in combination with the aromatase inhibitor letrozole (Kim et al. 2023), other data indicate an opposite role for CDK6 in regulating NET formation as $CDK6^{-/-}$ mice failed to produce NETs upon PMA stimulation (Amulic et al. 2017). Additionally, $CDK6^{-/-}$ mice exhibited a higher amount of primary granule proteins, suggesting CDK6 as a regulator of neutrophil granularity (Fleming et al. 2025). These data might explain the outcome seen in EBA.

The most efficient CDKi, MC180295, was next administered in two other models to verify the neutrophil-dependent effects: STA, which is neutrophil- and macrophage-dependent, and ITP, which is mostly neutrophil-independent. In STA, MC180295 significantly reduced disease severity and levels of several inflammatory cytokines. These findings complement a study describing protective effects on human chondrocytes and cartilage explants by CDK9 inhibition with flavopiridol or small interfering RNA. Less pro-inflammatory cytokines are released, preventing cartilage degradation (Yik et al. 2014).

Nevertheless, compared to the almost complete protection from disease development observed in the local antibody transfer-induced EBA model, the MC180295-treated STA mice showed a mean arthritis score of 2 on the final day, which represents still 22 % to that of the control mice in contrast to only 5 % in the EBA model. This finding might reflect the different functional relevance of neutrophils in the two distinct models. While EBA is described to be primarily neutrophil-driven (Chiriac et al. 2007), neutrophils also play a critical (Wipke and Allen 2001) yet not exclusive role in STA (Solomon et al. 2005). In the latter model, the function of macrophages during the effector phase of the disease is also well established (Christensen et al. 2016) and might explain the differences in efficacy seen on both models. A study conducted with LPS-stimulated human monocyte-derived macrophages demonstrated a reduction of IL-6 and TNF after treatment with AT7519 or roscovitine, supporting a role for macrophages in the resolution of inflammation (McHugh et al. 2022). In addition, CDK

inhibition may beneficially influence osteoclastogenesis, thereby reducing bone destruction in RA (Staniszewska et al. 2023).

Conversely, no effects on platelet depletion or recovery were observed in ITP. Contrasting with EBA and STA, neutrophils are considered dispensable for the effector phase of ITP. Rather other immune cells like macrophages or dendritic cells are involved (Zufferey et al. 2017). This highlights the role for CDK9 in IC-induced neutrophil-dependent diseases like EBA and STA.

Of note, the most efficiently inhibited kinases were CDK7, 9 and 11. Functions for all of these CDKs in transcriptional regulation have been described (Pellarin et al. 2025; Lim and Kaldis 2013). Accordingly, our data highlight that transcriptional changes are induced upon neutrophil IC-stimulation *in vitro* and functional changes become apparent. This is in line with our expectations considering that neutrophils are non-proliferating cells.

Regarding potential limitations of this study, only one concentration of each inhibitor was used *in vivo*. Thus, any effects which might be seen at different concentrations remain unclear. However, these concentrations had successfully been used in mouse models before and were hence deemed safe to apply. Additionally, only one inhibitor per target (except for CDK7 since both inhibitors were equally promising) was tested. We are aware that other inhibitors with different specificities or bioavailability might be more efficient, nevertheless the use of further inhibitors would have exceeded the scope of this explorative study. The way is now paved for further studies grounding on this work.

Instead of pharmacological inhibition, genetic knockouts could be a more precise alternative to address our research questions. Unfortunately, genetic deletions of many CDKs are embryonically lethal, with CDK1 being indispensable for early embryogenesis (Satyanarayana et al. 2008; Santamaría et al. 2007). CDK4- and CDK6-deficient mice display problems in embryonic development (Berthet et al. 2006; Malumbres et al. 2004) similar to $CDK8^{-/-}$ (Westerling et al. 2007), $CDK11^{-/-}$ (Li et al. 2004) or $CDK12^{-/-}$ mice (Juan et al. 2016). Therefore, we consider pharmacological inhibition to be a practicable and clinically relevant alternative, though future studies with neutrophil-specific inducible depletion may be informative.

Taken together, we have demonstrated the functional relevance of CDKs including CDK7, 9, and 11 in neutrophil IC-induced kinase signalling both *in vitro* and *in vivo*. Our findings contribute to the exploration of potential novel treatment options for autoimmune diseases such as PD or RA.

Acknowledgements

We thank Kathrin Kalies, Petra Lau, Astrid Fischer, Claudia Kauderer, Alexandra Wobig, Daniela Rieck, Norbert Reiling, Carolin Möller, and Cindy Jensen for their support.

Funding Statement

This research was funded by the Cluster of Excellence "Precision Medicine in Chronic Inflammation" (EXC 2167), the Research Training Group "Defining and Targeting Autoimmune Pre-Disease" (GRK 2633), and the Collaborative Research Center "Pathomechanisms of Antibody-mediated Autoimmunity" (CRC 1526), all from the Deutsche Forschungsgemeinschaft and the Schleswig-Holstein Excellence-Chair Program from the State of Schleswig Holstein.

Figure Legends

Fig. 1: Cell cycle and transcriptional *CDKs* are expressed in human neutrophils and IC-stimulation partially alters their expression. (**A**) Human neutrophils were purified and unstimulated cells (unstim) plus cells stimulated for 6 h with COL7 anti-COL7 IgG1-IC (6 h IC) were analysed by bulk RNAseq. Expression in unstimulated and stimulated neutrophils was compared for the individual *CDKs* on the basis of raw counts. **(B)** Significantly differentially expressed genes among CDKs, cyclins, and selected regulators were determined and log2 fold changes (log2 FC) are displayed for the individual samples. **(C)** Top 20 GO activated and suppressed pathways after gene set enrichment analysis of genes significantly differentially expressed upon IC stimulation. Adjusted p value (p. adjust) < 0.1. Gene ratio equals the ratio of differentially expressed genes in the given GO term, count refers to the absolute number. n = 3.

Fig. 2: *CDK2* and *4* expression are induced upon IC stimulation in human PMNs whereas *CDK9* and *19* are partly suppressed. (A) Human PMNs were isolated, stimulated for 6 h with COL7 anti-COL7 IgG1-IC and subjected to qRT-PCR detecting 14 distinct CDKs and CDC7 using the the $2^{-\Delta\Delta Ct}$ method. **(B)** In parallel, B cells and $CD4^+$ T cells were purified and analysed in the same way for comparison with unstimulated PMNs. n = 5. Mann-Whitney test **(A)** or Kruskal-Wallis test with Dunn's multiple comparisons test **(B)**. * $p \leq 0.05$. ** $p \leq 0.01$. *** $p \leq 0.001$.

Fig. 3: CDK7, 9, and 11 inhibition improve neutrophil effector functions and characteristics. Different neutrophil functions and characteristics were analysed after COL7 anti-COL7 IgG1-IC stimulation of human PMNs for 2 h and inhibition with three CDKi: **(A)** CD62L shedding, **(B)** CD18 expression, **(C)** adhesion, **(D)** ROS release, **(E)** apoptosis, and **(F)** viability. The results were normalised to the positive control without inhibitor indicated by the red line. The dose-response curves were calculated and the IC_{50}/EC_{50} values are indicated if in the tested concentration range. Cells only, antigen only (Ag), and antibody only (Ab) served as negative controls. Kruskal-Wallis test with Dunn's multiple comparisons test was performed. * $p \leq 0.05$. ** $p \leq 0.01$. *** $p \leq 0.001$. n = 5. AUC, area under the curve.

Fig. 4: Systemic and topical treatment with CDK7, 9, and 11 inhibitors improves disease severity in the local antibody-transfer induced EBA model. (A) EBA was induced by injection of anti-$mCOL7^c$ IgG and the mice were treated with CDKi either systemically or topically. **(B)** Exemplary clinical and histological images are shown with the scale bars corresponding to 100 µM. Asterisks indicate cell infiltrates and arrows indicate binding of C3/IgG to the dermal-epidermal junction. **(C)**

The affected ear surface area (AESA) and the H&E score were evaluated in the systemic treatment group for MC180295, **(D)** THZ2, **(E)** THZ1 2HCl, and **(F)** OTS964. **(G)** For the topical model, AESA was analysed as well. Two-way ANOVA with Šidák's multiple comparisons test was performed for AESA evaluation, except for the systemic treatment with THZ2 and MC180295 a mixed-effects analysis with Šidák's multiple comparisons test was conducted. For H&E scores, Mann-Whitney test was carried out. * $p \leq 0.05$. ** $p \leq 0.01$. **** $p \leq 0.0001$. n = 8.

Fig. 5: CDK9 inhibition with MC180295 improves disease severity in STA, but not in ITP. (A) To induce STA, mice were injected with KBxN serum and treated with MC180295 for seven days. **(B)** The course of the disease score is depicted and **(C)** reflected by the clinical presentation of the paws and the histological stainings. The scale bars represent 100 µM. Asterisks indicate proteoglycan staining (Safranin-O) or cell infiltration (H&E). **(D)** Cytokine levels were measured and significant results are shown. **(E)** ITP was induced by anti-platelet IgG2c-induced platelet depletion and MC180295 was applied starting 24 h before depletion until 24 hours post-injection (p.i.). **(F)** Absolute and **(G)** relative platelet counts normalised to 100 % at 0 h are indicated. For arthritis score and platelet counts, two-way ANOVA with Šidák's multiple comparisons test was performed. For cytokine levels, Mann-Whitey test was conducted. * $p \leq 0.05$. ** $p \leq 0.01$. **** $p \leq 0.0001$. **(A-D)** n = 5 (treatment) and n = 4 (control). **(E-G)** n = 4.

Fig. 6: Successful inhibition of neutrophil functions and experimental autoimmune models using CDKi. Out of 20 CDKs that are described in humans, 14 were detected in our gene expression analysis. After selecting specific CDKi, different *in vitro* neutrophil functional assays were performed. The number of efficient inhibitors is indicated. Subsequently, all CDKi that inhibited ROS release were tested as systemic treatment in the local antibody transfer-induced EBA model, except for BAY1251152 to avoid redundancy. Three CDKi reduced the disease severity and were thus applied topically in the same model. Additionally, the most promising CDKi was validated in STA and ITP.

Fig. S1: CDK1i Ro 3306 and CDK7i THZ1 2HCl reduce CD62L shedding in IC-stimulated human PMNs. (A-K) Human PMNs were stimulated for 2 h with hCOL7 anti-COL7 IgG1-IC and subsequently analysed for CD62L shedding. Inhibitors targeting specific CDKs were tested in flow cytometry for their ability to minimise CD62L shedding. Based on FSC-SSC gating, alive singlet $CD45^+$ cells were considered. The results were normalised to the positive control without inhibitor indicated by the red line. The dose-response curves were calculated and the IC_{50}/EC_{50} values are indicated if in the tested concentration range. Cells only, antigen only (Ag), and antibody only (Ab) served as negative controls. Kruskal-Wallis test with Dunn's multiple comparisons test was performed. * $p \leq 0.05$. ** $p \leq 0.01$. *** $p \leq 0.001$. n = 5.

Fig. S2: Inhibiting CDK1 by Ro 3306 or CDK7 by THZ1 2HCl decreases CD18 expression on IC-activated human PMNs. (A-K) Following stimulation of human PMNs for 2 h with hCOL7 anti-COL7 IgG1-IC and treatment with CDKi, the cells were analysed for their CD18 expression in flow cytometry. Based on FSC-SSC gating. alive singlet $CD45^+$ cells were considered. The results were normalised to the positive control without inhibitor indicated by the red line. The dose-response curves were calculated and the IC_{50} values are indicated if in the tested concentration range. Cells only,

antigen only (Ag), and antibody only (Ab) served as negative controls. Kruskal-Wallis test with Dunn's multiple comparisons test was performed. * $p \leq 0.05$. ** $p \leq 0.01$. n = 5.

Fig. S3: Adhesion of IC-activated human PMNs is not significantly reduced by the additional CDKi used. (A-K) Human PMNs were stimulated with hCOL7 anti-COL7 IgG1-IC for 2 h. Impedance-based measurement of adhesion was conducted using inhibitors targeting specific CDKs. The area under the curve was determined and the results were normalised to the positive control without inhibitor indicated by the red line. The dose-response curves were calculated and the IC_{50}/EC_{50} values are indicated if in the tested concentration range. Cells only, antigen only (Ag), and antibody only (Ab) served as negative controls. Kruskal-Wallis test with Dunn's multiple comparisons test was performed. * $p \leq 0.05$. ** $p \leq 0.01$. *** $p \leq 0.001$. n = 5.

Fig. S4: Inhibition of CDK1, 2, 4/6, 7, and 9 in IC-stimulated human PMNs minimises the ROS release. (A-K) Activation of human PMNs with hCOL7 anti-COL7 IgG1-IC for 2 h, treatment with specific CDKi and subsequent chemiluminescence-based analysis of ROS release was performed. The area under the curve (AUC) was calculated and the results were normalised to the positive control without inhibitor indicated by the red line. The dose-response curves were calculated and the IC_{50} values are indicated if in the tested concentration range. Cells only, antigen only (Ag), and antibody only (Ab) served as negative controls. Kruskal-Wallis test with Dunn's multiple comparisons test was performed. * $p \leq 0.05$. ** $p \leq 0.01$. *** $p \leq 0.001$. n = 5.

Fig. S5: Apoptosis in IC-stimulated human PMNs is increased by application of CDK1/2i, CDK12i, or CDK8/19i. (A-K) Human PMNs were activated with hCOL7 anti-COL7 IgG1-IC for 2 h. After using specific CDKi, flow cytometry was performed. Based on FSC-SSC gating, singlet $CD45^+$ cells were analysed. Annexin V^+ Zombie NIR^- cells were considered apoptotic. The results were normalised to the positive control without inhibitor indicated by the red line. The dose-response curves were calculated and the EC_{50} values are indicated if in the tested concentration range. Cells only, antigen only (Ag), and antibody only (Ab) served as negative controls. Kruskal-Wallis test with Dunn's multiple comparisons test was performed. * $p \leq 0.05$. ** $p \leq 0.01$. *** $p \leq 0.001$. n = 5.

Fig. S6: Viability of IC-treated human PMNs is minorly affected by CDK1, 7, and 12 inhibition at 10 µM. (A-K) Human PMNs stimulated with hCOL7 anti-COL7 IgG1-IC and treated with CDKi for 2 h were analysed for toxic effects in flow cytometry. Based on FSC-SSC gating, singlet $CD45^+$ cells were studied. Annexin V^- Zombie NIR^- cells were considered viable. The results were normalised to the positive control without inhibitor indicated by the red line. The dose-response curves were calculated and the IC_{50} values are indicated if in the tested concentration range. Cells only, antigen only (Ag), and antibody only (Ab) served as negative controls. Kruskal-Wallis test with Dunn's multiple comparisons test was performed. * $p \leq 0.05$. n = 5.

Fig. S7: CDK1 inhibition by Ro 3306 or CDK4/6 inhibition by palbociclib HCl does not reduce the affected ear surface area in local antibody-transfer-induced EBA. **(A-B)** EBA was induced by injection of anti-$mCOL7^c$ IgG and the mice were treated systemically with three more CDKi. The

affected ear surface area (AESA) was evaluated. Mixed-effects analysis with Šidák's multiple comparisons test was performed. *** $p \leq 0.001$. **(A)** n = 7, **(B)** n = 4.

Fig. S8: Additional cytokines are not influenced by MC180295 treatment in STA. (A-I) To induce STA. mice were injected with KBxN serum and treated with MC180295 for seven days. Further nine cytokines were analysed in the serum of STA mice and not significant results are shown. Two-way ANOVA with Šidák's multiple comparisons test was performed. n = 5 (treatment) and n = 4 (control).

References

Amulic, Borko, Sebastian Lorenz Knackstedt, Ulrike Abu Abed, et al. 2017. 'Cell-Cycle Proteins Control Production of Neutrophil Extracellular Traps'. *Developmental Cell* 43 (4): 449-462.e5. https://doi.org/10.1016/j.devcel.2017.10.013.

Arnaout, M. Amin. 2016. 'Biology and Structure of Leukocyte B2 Integrins and Their Role in Inflammation'. *F1000Research* 5 (October): 2433. https://doi.org/10.12688/f1000research.9415.1.

Aroca-Crevillén, Alejandra, Tommaso Vicanolo, Samuel Ovadia, and Andrés Hidalgo. 2024. 'Neutrophils in Physiology and Pathology'. *Annual Review of Pathology: Mechanisms of Disease* 19 (1): 227–59. https://doi.org/10.1146/annurev-pathmechdis-051222-015009.

Ashburner, Michael, Catherine A. Ball, Judith A. Blake, et al. 2000. 'Gene Ontology: Tool for the Unification of Biology'. *Nature Genetics* 25 (1): 25–29. https://doi.org/10.1038/75556.

Bajaj, Narinder P.S, Safa T Al-Sarraj, Valerie Anderson, Mavis Kibble, Nigel Leigh, and Christopher C.J Miller. 1998. 'Cyclin-Dependent Kinase-5 Is Associated with Lipofuscin in Motor Neurones in Amyotrophic Lateral Sclerosis'. *Neuroscience Letters* 245 (1): 45–48. https://doi.org/10.1016/S0304-3940(98)00176-1.

Beach, David, Barbara Durkacz, and Paul Nurse. 1982. 'Functionally Homologous Cell Cycle Control Genes in Budding and Fission Yeast'. *Nature* 300 (5894): 706–9. https://doi.org/10.1038/300706a0.

Berthet, Cyril, Kimberly D. Klarmann, Mary Beth Hilton, et al. 2006. 'Combined Loss of Cdk2 and Cdk4 Results in Embryonic Lethality and Rb Hypophosphorylation'. *Developmental Cell* 10 (5): 563–73. https://doi.org/10.1016/j.devcel.2006.03.004.

Bieber, Katja, Anna Lara Ernst, Stefan Tukaj, et al. 2017. 'Analysis of Serum Markers of Cellular Immune Activation in Patients with Bullous Pemphigoid'. *Experimental Dermatology* 26 (12): 1248–52. https://doi.org/10.1111/exd.13382.

Bieber, Katja, Mareike Witte, Shijie Sun, et al. 2016. 'T Cells Mediate Autoantibody-Induced Cutaneous Inflammation and Blistering in Epidermolysis Bullosa Acquisita'. *Scientific Reports* 6 (1): 38357. https://doi.org/10.1038/srep38357.

Bury, Marina, Benjamin Le Calvé, Gerardo Ferbeyre, Volker Blank, and Frédéric Lessard. 2021. ‘New Insights into CDK Regulators: Novel Opportunities for Cancer Therapy’. *Trends in Cell Biology* 31 (5): 331–44. https://doi.org/10.1016/j.tcb.2021.01.010.

Cao, Lihuan, Fang Chen, Xianmei Yang, Weijin Xu, Jun Xie, and Long Yu. 2014. ‘Phylogenetic Analysis of CDK and Cyclin Proteins in Premetazoan Lineages’. *BMC Evolutionary Biology* 14 (1): 10. https://doi.org/10.1186/1471-2148-14-10.

Chiriac, Mt, J Roesler, A Sindrilaru, K Scharffetter-Kochanek, D Zillikens, and C Sitaru. 2007. ‘NADPH Oxidase Is Required for Neutrophil-Dependent Autoantibody-Induced Tissue Damage’. *The Journal of Pathology* 212 (1): 56–65. https://doi.org/10.1002/path.2157.

Christensen, Anne D., Claus Haase, Andrew D. Cook, and John A. Hamilton. 2016. ‘K/BxN Serum-Transfer Arthritis as a Model for Human Inflammatory Arthritis’. *Frontiers in Immunology* 7: 213. https://doi.org/10.3389/fimmu.2016.00213.

Cicenas, Jonas, and Mindaugas Valius. 2011. ‘The CDK Inhibitors in Cancer Research and Therapy’. *Journal of Cancer Research and Clinical Oncology* 137 (10): 1409–18. https://doi.org/10.1007/s00432-011-1039-4.

Delvecchio, Manuela, Jonathan Gaucher, Carmen Aguilar-Gurrieri, Esther Ortega, and Daniel Panne. 2013. ‘Structure of the P300 Catalytic Core and Implications for Chromatin Targeting and HAT Regulation’. *Nature Structural & Molecular Biology* 20 (9): 1040–46. https://doi.org/10.1038/nsmb.2642.

Donner, Aaron J., Christopher C. Ebmeier, Dylan J. Taatjes, and Joaquín M. Espinosa. 2010. ‘CDK8 Is a Positive Regulator of Transcriptional Elongation within the Serum Response Network’. *Nature Structural & Molecular Biology* 17 (2): 194–201. https://doi.org/10.1038/nsmb.1752.

Draetta, Giulio, and David Beach. 1988. ‘Activation of Cdc2 Protein Kinase during Mitosis in Human Cells: Cell Cycle-Dependent Phosphorylation and Subunit Rearrangement’. *Cell* 54 (1): 17–26. https://doi.org/10.1016/0092-8674(88)90175-4.

Evans, Tom, Eric T. Rosenthal, Jim Youngblom, Dan Distel, and Tim Hunt. 1983. ‘Cyclin: A Protein Specified by Maternal mRNA in Sea Urchin Eggs That Is Destroyed at Each Cleavage Division’. *Cell* 33 (2): 389–96. https://doi.org/10.1016/0092-8674(83)90420-8.

Fisher, Robert P., Pei Jin, Holly M. Chamberlin, and David O. Morgan. 1995. ‘Alternative Mechanisms of CAK Assembly Require an Assembly Factor or an Activating Kinase’. *Cell* 83 (1): 47–57. https://doi.org/10.1016/0092-8674(95)90233-3.

Fisher, Robert P., and David O. Morgan. 1994. ‘A Novel Cyclin Associates with M015/CDK7 to Form the CDK-Activating Kinase’. *Cell* 78 (4): 713–24. https://doi.org/10.1016/0092-8674(94)90535-5.

Fleming, Kathryn, Kate Burley, Fernando Ponce-Garcia, et al. 2025. ‘Genome-Wide Association Analysis of Neutrophil Granularity Identifies CDK6 as a Regulator of Primary Granules’. *iScience* 28 (8): 113072. https://doi.org/10.1016/j.isci.2025.113072.

Fry, David W., Patricia J. Harvey, Paul R. Keller, et al. 2004. ‘Specific Inhibition of Cyclin-Dependent Kinase 4/6 by PD 0332991 and Associated Antitumor Activity in Human Tumor Xenografts’. *Molecular Cancer Therapeutics* 3 (11): 1427–38. https://doi.org/10.1158/1535-7163.1427.3.11.

Ghorbanalipoor, Saeedeh, Kazuko Matsumoto, Natalie Gross, et al. 2024. ‘High Throughput Screening Identifies Repurposable Drugs for Modulation of Innate and Acquired Immune Responses’. *Journal of Autoimmunity* 148 (September): 103302. https://doi.org/10.1016/j.jaut.2024.103302.

Greenlee-Wacker, Mallary C. 2016. ‘Clearance of Apoptotic Neutrophils and Resolution of Inflammation’. *Immunological Reviews* 273 (1): 357–70. https://doi.org/10.1111/imr.12453.

Griffin, J D, O Spertini, T J Ernst, et al. 1990. ‘Granulocyte-Macrophage Colony-Stimulating Factor and Other Cytokines Regulate Surface Expression of the Leukocyte Adhesion Molecule-1 on Human Neutrophils, Monocytes, and Their Precursors.’ *The Journal of Immunology* 145 (2): 576–84. https://doi.org/10.4049/jimmunol.145.2.576.

Gross, Natalie, Jana Marketon, Sadegh Mousavi, Kathrin Kalies, Ralf J. Ludwig, and Katja Bieber. 2024. ‘Inhibition of Interferon Gamma Impairs Induction of Experimental Epidermolysis Bullosa Acquisita’. *Frontiers in Immunology* 15: 1343299. https://doi.org/10.3389/fimmu.2024.1343299.

Harper, J. W., and S. J. Elledge. 1998. ‘The Role of Cdk7 in CAK Function, a Retro-Retrospective’. *Genes & Development* 12 (3): 285–89. https://doi.org/10.1101/gad.12.3.285.

Hsu, Alan Y., Decheng Wang, Sheng Liu, et al. 2019. ‘Phenotypical microRNA Screen Reveals a Noncanonical Role of CDK2 in Regulating Neutrophil Migration’. *Proceedings of the National Academy of Sciences* 116 (37): 18561–70. https://doi.org/10.1073/pnas.1905221116.

Huang, Tianlu, Xiwei Ding, Guifang Xu, et al. 2019. ‘CDK7 Inhibitor THZ1 Inhibits MCL1 Synthesis and Drives Cholangiocarcinoma Apoptosis in Combination with BCL2/BCL-XL Inhibitor ABT-263’. *Cell Death & Disease* 10 (8): 602. https://doi.org/10.1038/s41419-019-1831-7.

Jeffrey, Philip D., Lily Tong, and Nikola P. Pavletich. 2000. ‘Structural Basis of Inhibition of CDK–Cyclin Complexes by INK4 Inhibitors’. *Genes & Development* 14 (24): 3115–25. https://doi.org/10.1101/gad.851100.

Juan, H-C, Y Lin, H-R Chen, and M-J Fann. 2016. ‘Cdk12 Is Essential for Embryonic Development and the Maintenance of Genomic Stability’. *Cell Death & Differentiation* 23 (6): 1038–48. https://doi.org/10.1038/cdd.2015.157.

Kasprick, Anika, Katja Bieber, and Ralf J. Ludwig. 2019. ‘Drug Discovery for Pemphigoid Diseases’. *Current Protocols in Pharmacology* 84 (1): e55. https://doi.org/10.1002/cpph.55.

Kim, Chang Gon, Min Hwan Kim, Jee Hung Kim, et al. 2023. ‘On-Treatment Derived Neutrophil-to-Lymphocyte Ratio and Survival with Palbociclib and Endocrine Treatment: Analysis of a Multicenter Retrospective Cohort and the PALOMA-2/3

Study with Immune Correlates'. *Breast Cancer Research* 25 (1): 4. https://doi.org/10.1186/s13058-022-01601-4.

Koga, Hiroshi, Catherine Prost-Squarcioni, Hiroaki Iwata, Marcel F. Jonkman, Ralf J. Ludwig, and Katja Bieber. 2019. 'Epidermolysis Bullosa Acquisita: The 2019 Update'. *Frontiers in Medicine* 5 (January): 362. https://doi.org/10.3389/fmed.2018.00362.

Kridin, Khalaf, Diana Kneiber, Eric H. Kowalski, Manuel Valdebran, and Kyle T. Amber. 2019. 'Epidermolysis Bullosa Acquisita: A Comprehensive Review'. *Autoimmunity Reviews* 18 (8): 786–95. https://doi.org/10.1016/j.autrev.2019.06.007.

Kuhns, Douglas B., Debra A.Long Priel, and John I. Gallin. 1995. 'Loss of L-Selectin (CD62L) on Human Neutrophils Following Exudation in Vivo'. *Cellular Immunology* 164 (2): 306–10. https://doi.org/10.1006/cimm.1995.1174.

Kwiatkowski, Nicholas, Tinghu Zhang, Peter B. Rahl, et al. 2014. 'Targeting Transcription Regulation in Cancer with a Covalent CDK7 Inhibitor'. *Nature* 511 (7511): 616–20. https://doi.org/10.1038/nature13393.

Lahti, Jill M., Jialing Xiang, Lucie S. Heath, Dario Campana, and Vincent J. Kidd. 1995. 'PITSLRE Protein Kinase Activity Is Associated with Apoptosis'. *Molecular and Cellular Biology* 15 (1): 1–11. https://doi.org/10.1128/MCB.15.1.1.

Lee, David M., Daniel S. Friend, Michael F. Gurish, Christophe Benoist, Diane Mathis, and Michael B. Brenner. 2002. 'Mast Cells: A Cellular Link Between Autoantibodies and Inflammatory Arthritis'. *Science* 297 (5587): 1689–92. https://doi.org/10.1126/science.1073176.

Lee, Melanie G., and Paul Nurse. 1987. 'Complementation Used to Clone a Human Homologue of the Fission Yeast Cell Cycle Control Gene Cdc2'. *Nature* 327 (6117): 31–35. https://doi.org/10.1038/327031a0.

Leitch, A E, C D Lucas, J A Marwick, R Duffin, C Haslett, and A G Rossi. 2012. 'Cyclin-Dependent Kinases 7 and 9 Specifically Regulate Neutrophil Transcription and Their Inhibition Drives Apoptosis to Promote Resolution of Inflammation'. *Cell Death & Differentiation* 19 (12): 1950–61. https://doi.org/10.1038/cdd.2012.80.

Leitch, Ae, C Haslett, and Ag Rossi. 2009. 'Cyclin□dependent Kinase Inhibitor Drugs as Potential Novel Anti□inflammatory and Pro□resolution Agents'. *British Journal of Pharmacology* 158 (4): 1004–16. https://doi.org/10.1111/j.1476-5381.2009.00402.x.

Li, Tongyuan, Akira Inoue, Jill M. Lahti, and Vincent J. Kidd. 2004. 'Failure To Proliferate and Mitotic Arrest of CDK11$^{p110/p58}$ -Null Mutant Mice at the Blastocyst Stage of Embryonic Cell Development'. *Molecular and Cellular Biology* 24 (8): 3188–97. https://doi.org/10.1128/MCB.24.8.3188-3197.2004.

Lim, Shuhui, and Philipp Kaldis. 2013. 'Cdks, Cyclins and CKIs: Roles beyond Cell Cycle Regulation'. *Development* 140 (15): 3079–93. https://doi.org/10.1242/dev.091744.

Liu, Z, G J Giudice, X Zhou, et al. 1997. 'A Major Role for Neutrophils in Experimental Bullous Pemphigoid.' *Journal of Clinical Investigation* 100 (5): 1256–63. https://doi.org/10.1172/JCI119639.

Livak, Kenneth J., and Thomas D. Schmittgen. 2001. ‘Analysis of Relative Gene Expression Data Using Real-Time Quantitative PCR and the 2−ΔΔCT Method’. *Methods* 25 (4): 402–8. https://doi.org/10.1006/meth.2001.1262.

Love, Michael I, Wolfgang Huber, and Simon Anders. 2014. ‘Moderated Estimation of Fold Change and Dispersion for RNA-Seq Data with DESeq2’. *Genome Biology* 15 (12): 550. https://doi.org/10.1186/s13059-014-0550-8.

Malumbres, Marcos. 2014. ‘Cyclin-Dependent Kinases’. *Genome Biology* 15 (6): 122. https://doi.org/10.1186/gb4184.

Malumbres, Marcos, Rocío Sotillo, David Santamaría, et al. 2004. ‘Mammalian Cells Cycle without the D-Type Cyclin-Dependent Kinases Cdk4 and Cdk6’. *Cell* 118 (4): 493–504. https://doi.org/10.1016/j.cell.2004.08.002.

Matsumoto, Daisuke, Beni Amatya, Daisuke Tsuruta, and Sho Hiroyasu. 2024. ‘The Pathological Function of Neutrophils in Pemphigoid Diseases’. *Dermatologica Sinica* 42 (2): 80–88. https://doi.org/10.4103/ds.DS-D-24-00027.

Matsuo, Yo, Jae-Hyun Park, Takashi Miyamoto, et al. 2014. ‘TOPK Inhibitor Induces Complete Tumor Regression in Xenograft Models of Human Cancer through Inhibition of Cytokinesis’. *Science Translational Medicine* 6 (259). https://doi.org/10.1126/scitranslmed.3010277.

McHugh, Brian J., Jillian Stephen, Calum T. Robb, et al. 2022. ‘Inhibition of Cyclin-Dependent Kinase 9 Downregulates Cytokine Production Without Detrimentally Affecting Human Monocyte-Derived Macrophage Viability’. *Frontiers in Cell and Developmental Biology* 10 (May): 905315. https://doi.org/10.3389/fcell.2022.905315.

McInnes, Iain B., and Georg Schett. 2011. ‘The Pathogenesis of Rheumatoid Arthritis’. *New England Journal of Medicine* 365 (23): 2205–19. https://doi.org/10.1056/NEJMra1004965.

Nigrovic, Peter A., Bryce A. Binstadt, Paul A. Monach, et al. 2007. ‘Mast Cells Contribute to Initiation of Autoantibody-Mediated Arthritis via IL-1’. *Proceedings of the National Academy of Sciences* 104 (7): 2325–30. https://doi.org/10.1073/pnas.0610852103.

Nilson, Kyle A., Jiannan Guo, Michael E. Turek, et al. 2015. ‘THZ1 Reveals Roles for Cdk7 in Co-Transcriptional Capping and Pausing’. *Molecular Cell* 59 (4): 576–87. https://doi.org/10.1016/j.molcel.2015.06.032.

Nurse, Paul. 2000. ‘A Long Twentieth Century of the Cell Cycle and Beyond’. *Cell* 100 (1): 71–78. https://doi.org/10.1016/S0092-8674(00)81684-0.

Nurse, Paul, Pierre Thuriaux, and Kim Nasmyth. 1976. ‘Genetic Control of the Cell Division Cycle in the Fission Yeast Schizosaccharomyces Pombe’. *Molecular and General Genetics MGG* 146 (2): 167–78. https://doi.org/10.1007/BF00268085.

Ogryzko, Vasily V, R.Louis Schiltz, Valya Russanova, Bruce H Howard, and Yoshihiro Nakatani. 1996. ‘The Transcriptional Coactivators P300 and CBP Are Histone Acetyltransferases’. *Cell* 87 (5): 953–59. https://doi.org/10.1016/S0092-8674(00)82001-2.

Parker, Laura L., and Helen Piwnica-Worms. 1992. ‘Inactivation of the P34 ^{cdc2} -Cyclin B Complex by the Human WEE1 Tyrosine Kinase’. *Science* 257 (5078): 1955–57. https://doi.org/10.1126/science.1384126.

Pavletich, Nikola P. 1999. ‘Mechanisms of Cyclin-Dependent Kinase Regulation: Structures of Cdks, Their Cyclin Activators, and Cip and INK4 Inhibitors’. *Journal of Molecular Biology* 287 (5): 821–28. https://doi.org/10.1006/jmbi.1999.2640.

Peissert, Stefan, Andreas Schlosser, Rafaela Kendel, Jochen Kuper, and Caroline Kisker. 2020. ‘Structural Basis for CDK7 Activation by MAT1 and Cyclin H’. *Proceedings of the National Academy of Sciences* 117 (43): 26739–48. https://doi.org/10.1073/pnas.2010885117.

Pellarin, Ilenia, Alessandra Dall’Acqua, Andrea Favero, et al. 2025. ‘Cyclin-Dependent Protein Kinases and Cell Cycle Regulation in Biology and Disease’. *Signal Transduction and Targeted Therapy* 10 (1): 11. https://doi.org/10.1038/s41392-024-02080-z.

Pluta, Aleksandra J., Cécilia Studniarek, Shona Murphy, and Chris J. Norbury. 2024. ‘Cyclin dependent Kinases: Masters of the Eukaryotic Universe’. *WIREs RNA* 15 (1): e1816. https://doi.org/10.1002/wrna.1816.

Recke, Andreas, Luisa M. Trog, Hendri H. Pas, et al. 2014. ‘Recombinant Human IgA1 and IgA2 Autoantibodies to Type VII Collagen Induce Subepidermal Blistering Ex Vivo’. *The Journal of Immunology* 193 (4): 1600–1608. https://doi.org/10.4049/jimmunol.1400160.

Rosales, Jesusa L., Joel D. Ernst, Janice Hallows, and Ki-Young Lee. 2004. ‘GTP-Dependent Secretion from Neutrophils Is Regulated by Cdk5’. *Journal of Biological Chemistry* 279 (52): 53932–36. https://doi.org/10.1074/jbc.M408467200.

Rossi, Adriano G, Deborah A Sawatzky, Annemieke Walker, et al. 2006. ‘Cyclin-Dependent Kinase Inhibitors Enhance the Resolution of Inflammation by Promoting Inflammatory Cell Apoptosis’. *Nature Medicine* 12 (9): 1056–64. https://doi.org/10.1038/nm1468.

Russo, Alicia A., Philip D. Jeffrey, and Nikola P. Pavletich. 1996. ‘Structural Basis of Cyclin-Dependent Kinase Activation by Phosphorylation’. *Nature Structural & Molecular Biology* 3 (8): 696–700. https://doi.org/10.1038/nsb0896-696.

Samavedam, Unni K., Nina Mitschker, Anika Kasprick, et al. 2018. ‘Whole-Genome Expression Profiling in Skin Reveals SYK As a Key Regulator of Inflammation in Experimental Epidermolysis Bullosa Acquisita’. *Frontiers in Immunology* 9 (February): 249. https://doi.org/10.3389/fimmu.2018.00249.

Sanidas, Ioannis, Michael S. Lawrence, and Nicholas J. Dyson. 2024. ‘Patterns in the Tapestry of Chromatin-Bound RB’. *Trends in Cell Biology* 34 (4): 288–98. https://doi.org/10.1016/j.tcb.2023.07.012.

Santamaría, David, Cédric Barrière, Antonio Cerqueira, et al. 2007. ‘Cdk1 Is Sufficient to Drive the Mammalian Cell Cycle’. *Nature* 448 (7155): 811–15. https://doi.org/10.1038/nature06046.

Satyanarayana, Ande, Cyril Berthet, Javier Lopez-Molina, Vincenzo Coppola, Lino Tessarollo, and Philipp Kaldis. 2008. 'Genetic Substitution of Cdk1 by Cdk2 Leads to Embryonic Lethality and Loss of Meiotic Function of Cdk2'. *Development* 135 (20): 3389–400. https://doi.org/10.1242/dev.024919.

Savill, J S, A H Wyllie, J E Henson, M J Walport, P M Henson, and C Haslett. 1989. 'Macrophage Phagocytosis of Aging Neutrophils in Inflammation. Programmed Cell Death in the Neutrophil Leads to Its Recognition by Macrophages.' *Journal of Clinical Investigation* 83 (3): 865–75. https://doi.org/10.1172/JCI113970.

Schmidt, Enno, and Detlef Zillikens. 2013. 'Pemphigoid Diseases'. *The Lancet* 381 (9863): 320–32. https://doi.org/10.1016/S0140-6736(12)61140-4.

Schwartz, Phillip A., and Brion W. Murray. 2011. 'Protein Kinase Biochemistry and Drug Discovery'. *Bioorganic Chemistry* 39 (5–6): 192–210. https://doi.org/10.1016/j.bioorg.2011.07.004.

Seeling, Michaela, Ulrike Hillenhoff, Jean Pierre David, et al. 2013. 'Inflammatory Monocytes and Fcγ Receptor IV on Osteoclasts Are Critical for Bone Destruction during Inflammatory Arthritis in Mice'. *Proceedings of the National Academy of Sciences* 110 (26): 10729–34. https://doi.org/10.1073/pnas.1301001110.

Seeling, Michaela, Matthias Pöhnl, Sibel Kara, et al. 2023. 'Immunoglobulin G-Dependent Inhibition of Inflammatory Bone Remodeling Requires Pattern Recognition Receptor Dectin-1'. *Immunity* 56 (5): 1046-1063.e7. https://doi.org/10.1016/j.immuni.2023.02.019.

Sitaru, Cassian, Sidonia Mihai, Christoph Otto, et al. 2005. 'Induction of Dermal-Epidermal Separation in Mice by Passive Transfer of Antibodies Specific to Type VII Collagen'. *Journal of Clinical Investigation* 115 (4): 870–78. https://doi.org/10.1172/JCI200521386.

Skoog, William A., and William S. Beck. 1956. 'Studies on the Fibrinogen, Dextran and Phytohemagglutinin Methods of Isolating Leukocytes'. *Blood* 11 (5): 436–54. https://doi.org/10.1182/blood.V11.5.436.436.

Solomon, M J, T Lee, and M W Kirschner. 1992. 'Role of Phosphorylation in P34cdc2 Activation: Identification of an Activating Kinase.' *Molecular Biology of the Cell* 3 (1): 13–27. https://doi.org/10.1091/mbc.3.1.13.

Solomon, Samuel, Narendiran Rajasekaran, Elvira Jeisy Walder, Scott B. Snapper, and Harald Illges. 2005. 'A Crucial Role for Macrophages in the Pathology of K/B × N Serum induced Arthritis'. *European Journal of Immunology* 35 (10): 3064–73. https://doi.org/10.1002/eji.200526167.

Staniszewska, Marzena, Kajetan Kiełbowski, Klaudia Rusińska, Estera Bakinowska, Ewa Gromowska, and Andrzej Pawlik. 2023. 'Targeting Cyclin-Dependent Kinases in Rheumatoid Arthritis and Psoriasis – a Review of Current Evidence'. *Expert Opinion on Therapeutic Targets* 27 (11): 1097–113. https://doi.org/10.1080/14728222.2023.2285784.

Stüssel, Pia, Katharina Schulze Dieckhoff, Sven Künzel, et al. 2020. 'Propranolol Is an Effective Topical and Systemic Treatment Option for Experimental Epidermolysis

Bullosa Acquisita'. *Journal of Investigative Dermatology* 140 (12): 2408–20. https://doi.org/10.1016/j.jid.2020.04.025.

Syahirah, Ramizah, Alan Y Hsu, and Qing Deng. 2022. 'A Curious Case of Cyclin-Dependent Kinases in Neutrophils'. *Journal of Leukocyte Biology* 111 (5): 1057–68. https://doi.org/10.1002/JLB.2RU1021-573R.

Tassan, J P, S J Schultz, J Bartek, and E A Nigg. 1994. 'Cell Cycle Analysis of the Activity, Subcellular Localization, and Subunit Composition of Human CAK (CDK-Activating Kinase).' *The Journal of Cell Biology* 127 (2): 467–78. https://doi.org/10.1083/jcb.127.2.467.

The Gene Ontology Consortium, Suzi A Aleksander, James Balhoff, et al. 2023. 'The Gene Ontology Knowledgebase in 2023'. *GENETICS* 224 (1): iyad031. https://doi.org/10.1093/genetics/iyad031.

Uhlén, Mathias, Linn Fagerberg, Björn M. Hallström, et al. 2015. 'Proteomics. Tissue-Based Map of the Human Proteome'. *Science (New York, N.Y.)* 347 (6220): 1260419. https://doi.org/10.1126/science.1260419.

Wang, Keqing, Peter Hampson, Jon Hazeldine, et al. 2012. 'Cyclin-Dependent Kinase 9 Activity Regulates Neutrophil Spontaneous Apoptosis'. *PLoS ONE* 7 (1): e30128. https://doi.org/10.1371/journal.pone.0030128.

Wang, Yubao, Tinghu Zhang, Nicholas Kwiatkowski, et al. 2015. 'CDK7-Dependent Transcriptional Addiction in Triple-Negative Breast Cancer'. *Cell* 163 (1): 174–86. https://doi.org/10.1016/j.cell.2015.08.063.

Westerling, Thomas, Emilia Kuuluvainen, and Tomi P. Maäkelaä. 2007. 'Cdk8 Is Essential for Preimplantation Mouse Development'. *Molecular and Cellular Biology* 27 (17): 6177–82. https://doi.org/10.1128/MCB.01302-06.

Wipke, Brian T., and Paul M. Allen. 2001. 'Essential Role of Neutrophils in the Initiation and Progression of a Murine Model of Rheumatoid Arthritis'. *The Journal of Immunology* 167 (3): 1601–8. https://doi.org/10.4049/jimmunol.167.3.1601.

Wöhner, Miriam, Sarah Brechtelsbauer, Niklas Friedrich, et al. 2024. 'Tissue Niche Occupancy Determines the Contribution of Fetal- versus Bone-Marrow-Derived Macrophages to IgG Effector Functions'. *Cell Reports* 43 (2): 113757. https://doi.org/10.1016/j.celrep.2024.113757.

Woodley, D T, R E Burgeson, G Lunstrum, L Bruckner-Tuderman, M J Reese, and R A Briggaman. 1988. 'Epidermolysis Bullosa Acquisita Antigen Is the Globular Carboxyl Terminus of Type VII Procollagen.' *Journal of Clinical Investigation* 81 (3): 683–87. https://doi.org/10.1172/JCI113373.

Wright, Helen L., Robert J. Moots, and Steven W. Edwards. 2014. 'The Multifactorial Role of Neutrophils in Rheumatoid Arthritis'. *Nature Reviews Rheumatology* 10 (10): 593–601. https://doi.org/10.1038/nrrheum.2014.80.

Wu, Chuan Xing, Xiao Qi Wang, Siu Ho Chok, et al. 2018. 'Blocking CDK1/PDK1/β-Catenin Signaling by CDK1 Inhibitor RO3306 Increased the Efficacy of Sorafenib Treatment

by Targeting Cancer Stem Cells in a Preclinical Model of Hepatocellular Carcinoma'. *Theranostics* 8 (14): 3737–50. https://doi.org/10.7150/thno.25487.

Wu, Lingling, Yuting Qin, Shiwei Xia, et al. 2016. 'Identification of Cyclin Dependent Kinase 1 as a Novel Regulator of Type I Interferon Signaling in Systemic Lupus Erythematosus'. *Arthritis & Rheumatology* 68 (5): 1222–32. https://doi.org/10.1002/art.39543.

Yang, Jinming, Weifeng Luo, Patricia Ward, et al. 2025. 'Combined Treatment with CDK4/6, CDK2, and CXCR1/2 Inhibitors Effectively Halts the Growth of BRAF Wild-Type Melanoma Tumors'. *Frontiers in Oncology* 15 (August): 1609735. https://doi.org/10.3389/fonc.2025.1609735.

Yang, Kai, Junping Yin, Xiaoyang Yue, et al. 2023. 'Luteolin Peracetate and Gossypolone Inhibit Immune Complex-Mediated Neutrophil Activation in Vitro and Dermal-Epidermal Separation in an Ex Vivo Model of Epidermolysis Bullosa Acquisita'. *Frontiers in Immunology* 14 (September): 1196116. https://doi.org/10.3389/fimmu.2023.1196116.

Yik, Jasper H. N., Zi'ang Hu, Ratna Kumari, Blaine A. Christiansen, and Dominik R. Haudenschild. 2014. 'Cyclin Dependent Kinase 9 Inhibition Protects Cartilage From the Catabolic Effects of Proinflammatory Cytokines'. *Arthritis & Rheumatology* 66 (6): 1537–46. https://doi.org/10.1002/art.38378.

Yu, Xinhua, Reza Akbarzadeh, Mario Pieper, et al. 2018. 'Neutrophil Adhesion Is a Prerequisite for Antibody-Mediated Proteolytic Tissue Damage in Experimental Models of Epidermolysis Bullosa Acquisita'. *Journal of Investigative Dermatology* 138 (9): 1990–98. https://doi.org/10.1016/j.jid.2018.03.1499.

Zarrin, Ali A., Katherine Bao, Patrick Lupardus, and Domagoj Vucic. 2021. 'Kinase Inhibition in Autoimmunity and Inflammation'. *Nature Reviews Drug Discovery* 20 (1): 39–63. https://doi.org/10.1038/s41573-020-0082-8.

Zhang, Hanghang, Somnath Pandey, Meghan Travers, et al. 2018. 'Targeting CDK9 Reactivates Epigenetically Silenced Genes in Cancer'. *Cell* 175 (5): 1244-1258.e26. https://doi.org/10.1016/j.cell.2018.09.051.

Zhang, Mengna, Lingxian Zhang, Ruoxuan Hei, et al. 2021. 'CDK Inhibitors in Cancer Therapy, an Overview of Recent Development'. *American Journal of Cancer Research* 11 (5): 1913–35.

Zhang, Xiaozhu, Lily Ding, and Andrew J Sandford. 2005. 'Selection of Reference Genes for Gene Expression Studies in Human Neutrophils by Real-Time PCR'. *BMC Molecular Biology* 6 (1): 4. https://doi.org/10.1186/1471-2199-6-4.

Zillikens, Hannah, Anika Kasprick, Colin Osterloh, et al. 2021. 'Topical Application of the PI3Kβ-Selective Small Molecule Inhibitor TGX-221 Is an Effective Treatment Option for Experimental Epidermolysis Bullosa Acquisita'. *Frontiers in Medicine* 8 (September): 713312. https://doi.org/10.3389/fmed.2021.713312.

Zufferey, Anne, Rick Kapur, and John Semple. 2017. 'Pathogenesis and Therapeutic Mechanisms in Immune Thrombocytopenia (ITP)'. *Journal of Clinical Medicine* 6 (2): 16. https://doi.org/10.3390/jcm6020016.

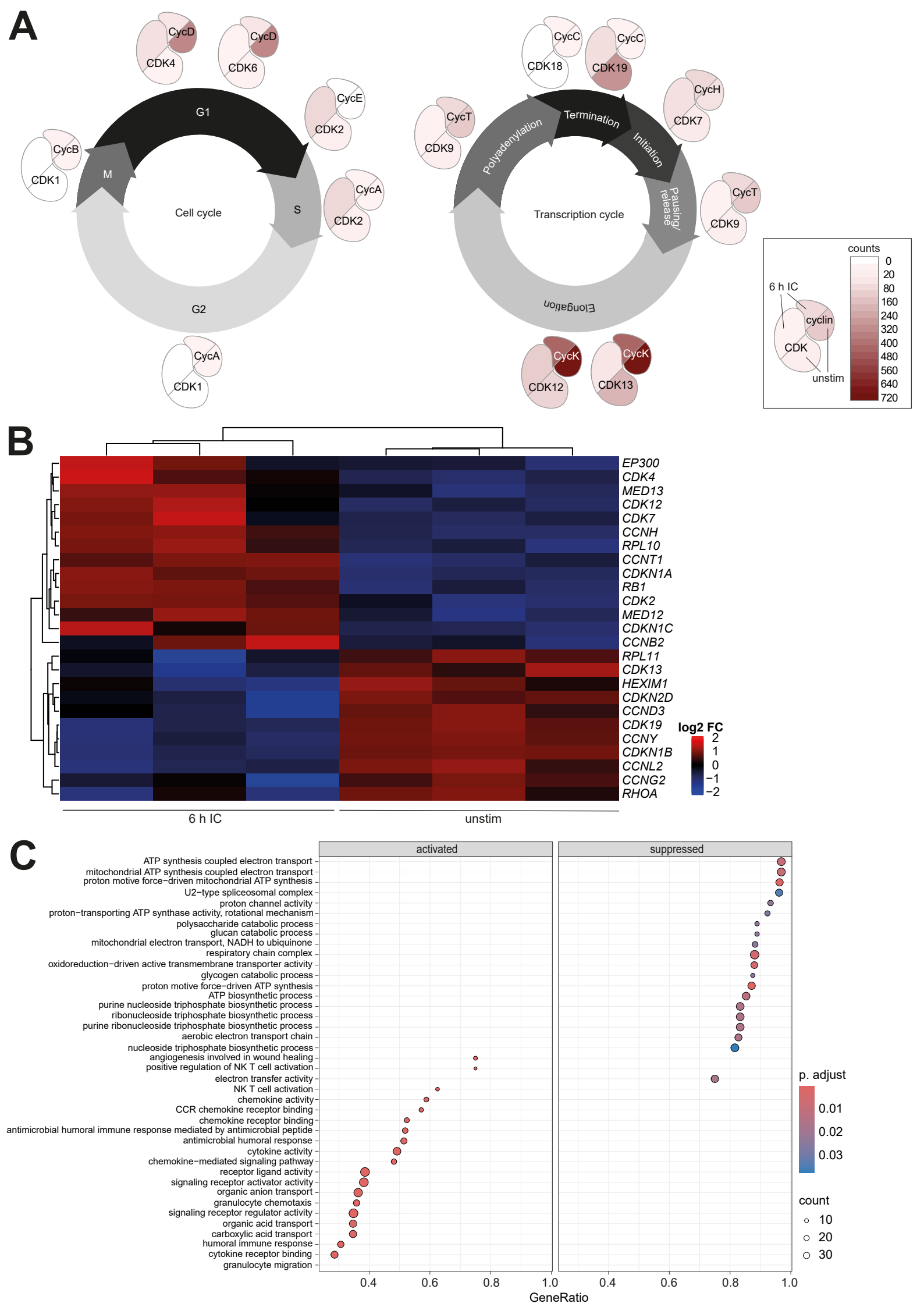
A
CycD
CDK4
CycD
CDK6
CycE
CDK2
CycB
CDK1
G1
M
S
Cell cycle
CycA
CDK2
G2
CycA
CDK1
CycC
CDK18
CycC
CDK19
CycH
CDK7
CycT
CDK9
Termination
Polyadenylation
Initiation
Pausing/ release
Transcription cycle
CycT
CDK9
Elongation
CycK
CDK12
CycK
CDK13
counts
0
20
80
160
240
320
400
480
560
640
720
6 h IC
cyclin
CDK
unstim
B
EP300
CDK4
MED13
CDK12
CDK7
CCNH
RPL10
CCNT1
CDKN1A
RB1
CDK2
MED12
CDKN1C
CCNB2
RPL11
CDK13
HEXIM1
CDKN2D
CCND3
CDK19
CCNY
CDKN1B
CCNL2
CCNG2
RHOA
log2 FC
2
1
0
−1
−2
6 h IC
unstim
C
activated
suppressed
ATP synthesis coupled electron transport
mitochondrial ATP synthesis coupled electron transport
proton motive force−driven mitochondrial ATP synthesis
U2−type spliceosomal complex
proton channel activity
proton−transporting ATP synthase activity, rotational mechanism
polysaccharide catabolic process
glucan catabolic process
mitochondrial electron transport, NADH to ubiquinone
respiratory chain complex
oxidoreduction−driven active transmembrane transporter activity
glycogen catabolic process
proton motive force−driven ATP synthesis
ATP biosynthetic process
purine nucleoside triphosphate biosynthetic process
ribonucleoside triphosphate biosynthetic process
purine ribonucleoside triphosphate biosynthetic process
aerobic electron transport chain
nucleoside triphosphate biosynthetic process
angiogenesis involved in wound healing
positive regulation of NK T cell activation
electron transfer activity
NK T cell activation
chemokine activity
CCR chemokine receptor binding
chemokine receptor binding
antimicrobial humoral immune response mediated by antimicrobial peptide
antimicrobial humoral response
cytokine activity
chemokine−mediated signaling pathway
receptor ligand activity
signaling receptor activator activity
organic anion transport
granulocyte chemotaxis
signaling receptor regulator activity
organic acid transport
carboxylic acid transport
humoral immune response
cytokine receptor binding
granulocyte migration
0.4
0.6
0.8
1.0
GeneRatio
p. adjust
0.01
0.02
0.03
count
10
20
30

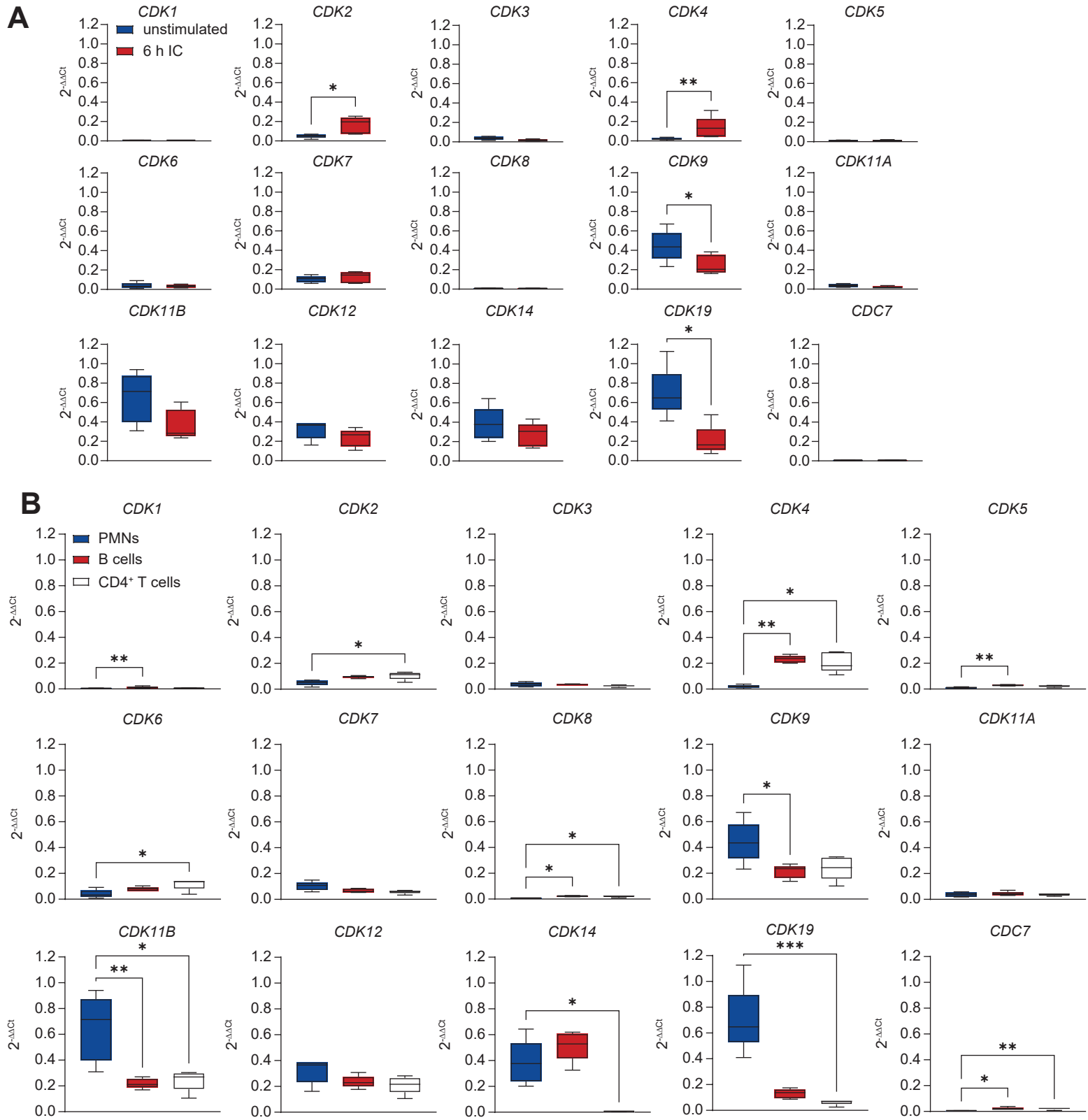
A
CDK1
CDK2
CDK3
CDK4
CDK5
CDK6
CDK7
CDK8
CDK9
CDK11A
CDK11B
CDK12
CDK14
CDK19
CDC7
unstimulated
6 h IC
2-ΔΔCt
B
PMNs
B cells
CD4+ T cells

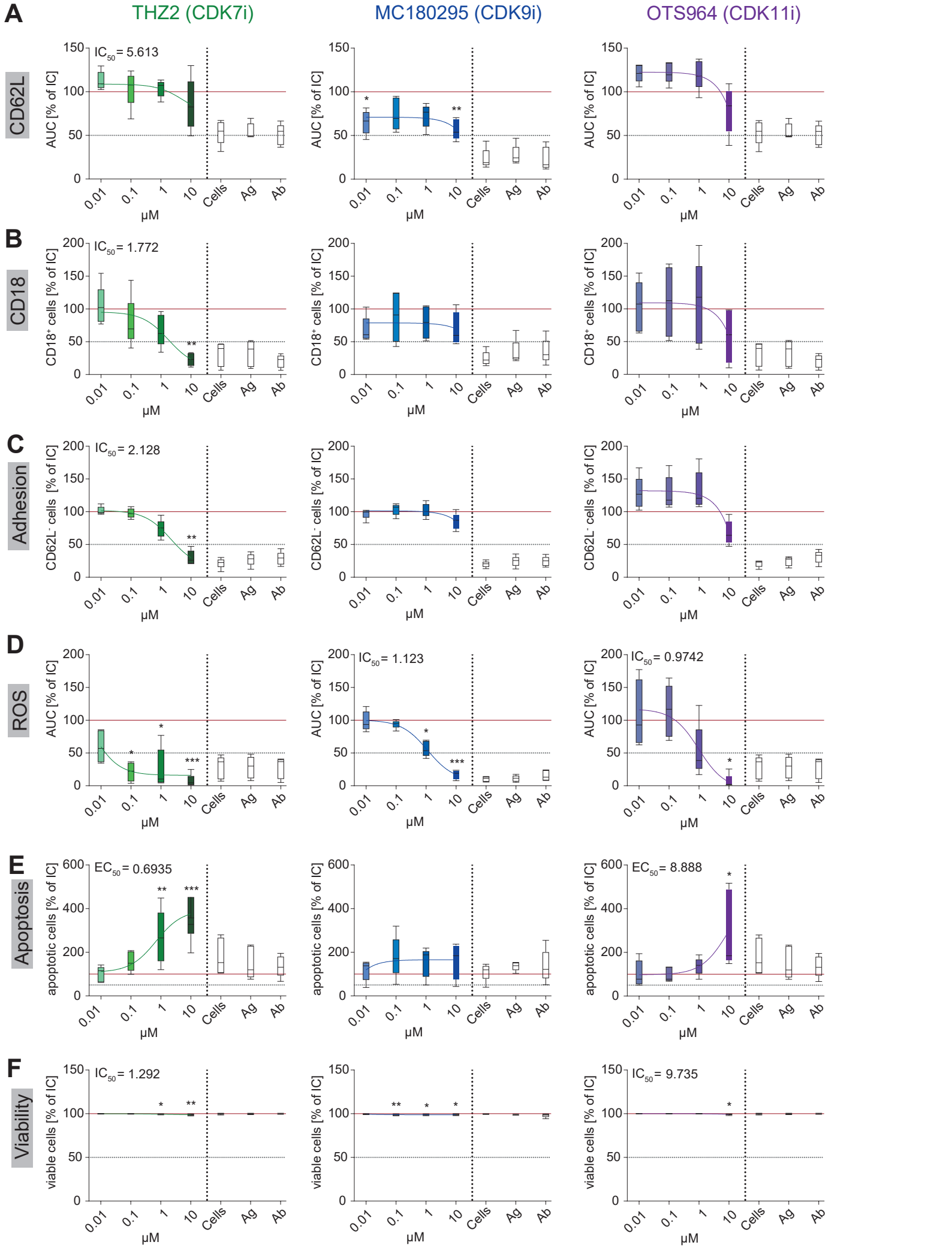
A
THZ2 (CDK7i)
MC180295 (CDK9i)
OTS964 (CDK11i)
CD62L
AUC [% of IC]
IC50 = 5.613
IC50 = 1.123
IC50 = 0.9742
B
CD18
CD18+ cells [% of IC]
IC50 = 1.772
C
Adhesion
CD62L- cells [% of IC]
IC50 = 2.128
D
ROS
AUC [% of IC]
IC50 = 1.123
IC50 = 0.9742
E
Apoptosis
apoptotic cells [% of IC]
EC50 = 0.6935
EC50 = 8.888
F
Viability
viable cells [% of IC]
IC50 = 1.292
IC50 = 9.735
0.01
0.1
1
10
Cells
Ag
Ab
µM

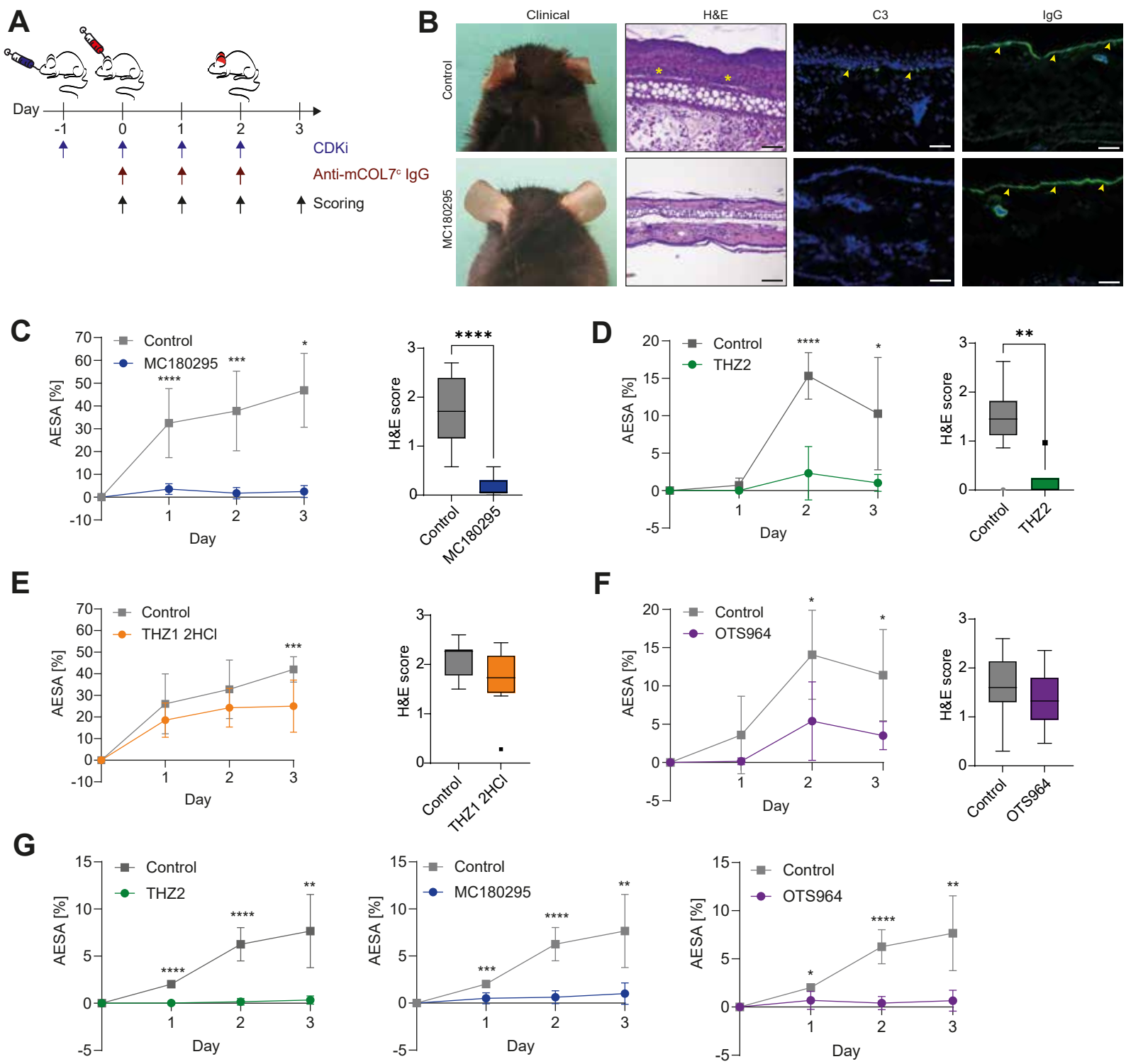
A
Day
-1
0
1
2
3
CDKi
Anti-mCOL7c IgG
Scoring
B
Clinical
H&E
C3
IgG
Control
MC180295
C
Control
MC180295
AESA [%]
Day
H&E score
Control
MC180295
D
Control
THZ2
AESA [%]
Day
H&E score
Control
THZ2
E
Control
THZ1 2HCl
AESA [%]
Day
H&E score
Control
THZ1 2HCl
F
Control
OTS964
AESA [%]
Day
H&E score
Control
OTS964
G
Control
THZ2
AESA [%]
Day
Control
MC180295
AESA [%]
Day
Control
OTS964
AESA [%]
Day

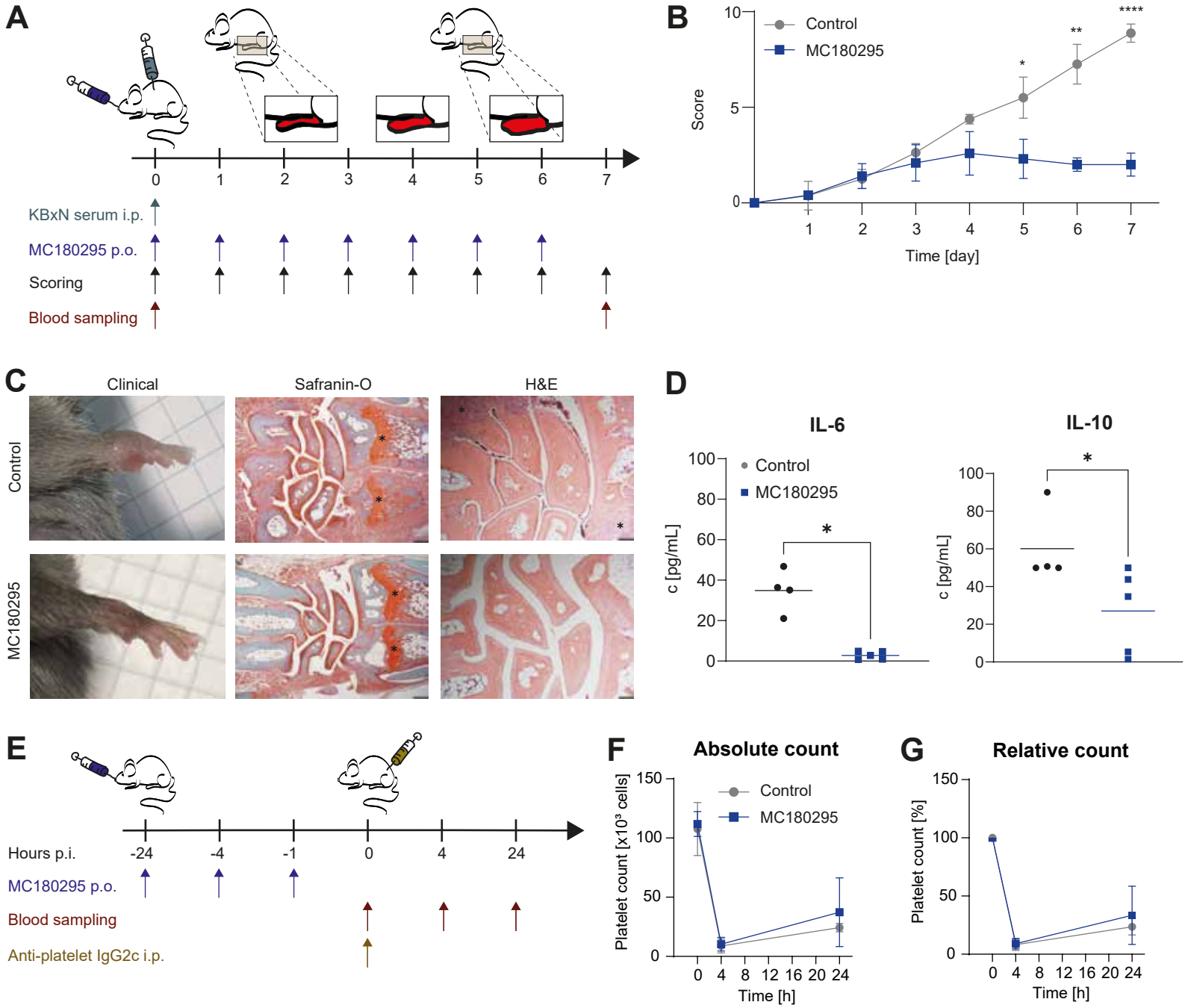
A
0
1
2
3
4
5
6
7
KBxN serum i.p.
MC180295 p.o.
Scoring
Blood sampling
B
Control
MC180295
Score
Time [day]
C
Clinical
Safranin-O
H&E
Control
MC180295
D
IL-6
IL-10
Control
MC180295
c [pg/mL]
E
Hours p.i.
-24
-4
-1
0
4
24
MC180295 p.o.
Blood sampling
Anti-platelet IgG2c i.p.
F
Absolute count
Control
MC180295
Platelet count [x10³ cells]
Time [h]
G
Relative count
Platelet count [%]
Time [h]

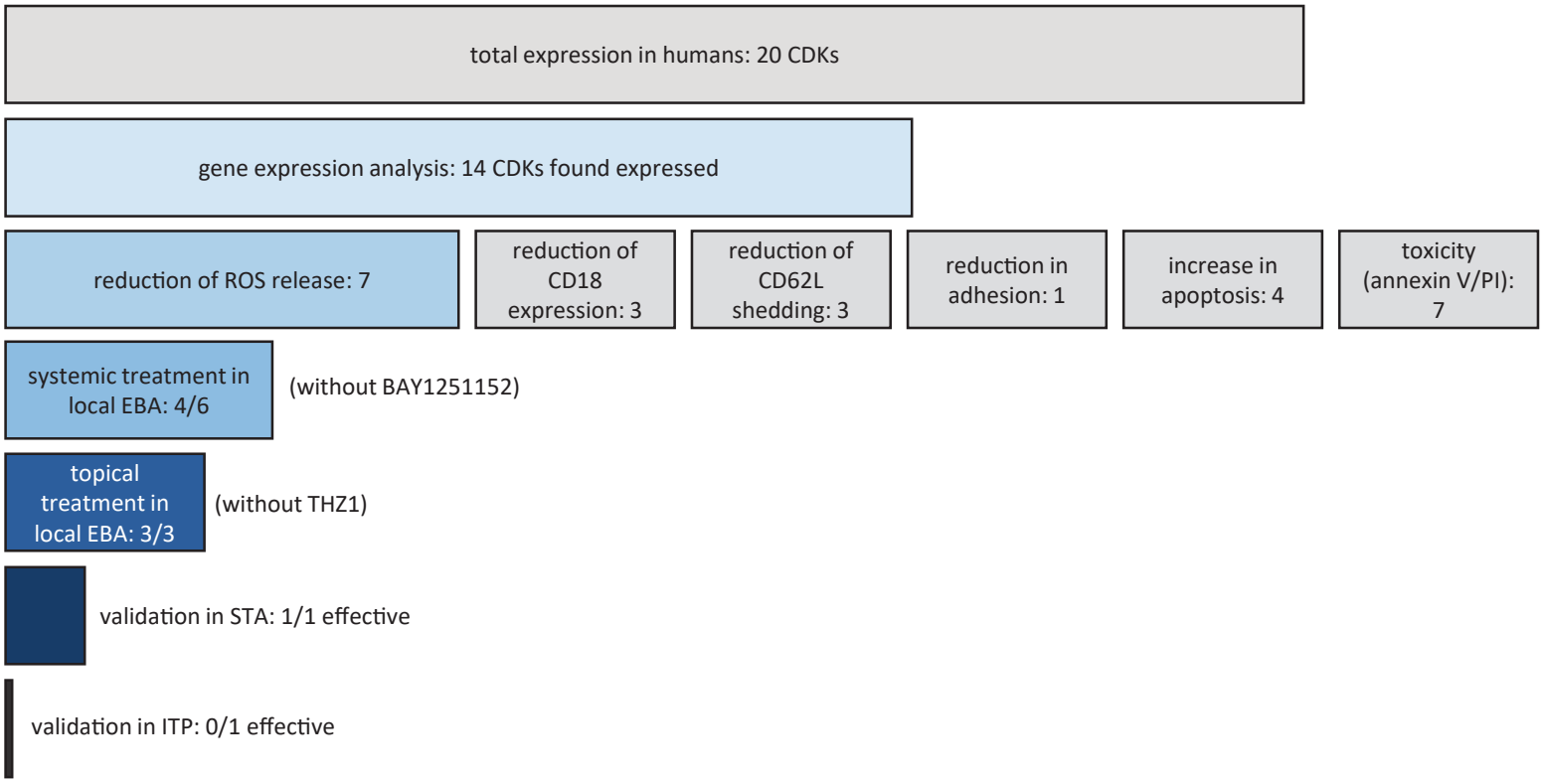
total expression in humans: 20 CDKs
gene expression analysis: 14 CDKs found expressed
reduction of ROS release: 7
reduction of CD18 expression: 3
reduction of CD62L shedding: 3
reduction in adhesion: 1
increase in apoptosis: 4
toxicity (annexin V/PI): 7
systemic treatment in local EBA: 4/6
(without BAY1251152)
topical treatment in local EBA: 3/3
(without THZ1)
validation in STA: 1/1 effective
validation in ITP: 0/1 effective